INFORMATION TO USERS

This manuscript has been reproduced from the microfilm master. UMI films the text directly from the original or copy submitted. Thus, some thesis and dissertation copies are in typewriter face, while others may be from any type of computer printer.

The quality of this reproduction is dependent upon the quality of the copy submitted. Broken or indistinct print, colored or poor quality illustrations and photographs, print bleedthrough, substandard margins, and improper alignment can adversely affect reproduction.

In the unlikely event that the author did not send UMI a complete manuscript and there are missing pages, these will be noted. Also, if unauthorized copyright material had to be removed, a note will indicate the deletion.

Oversize materials (e.g., maps, drawings, charts) are reproduced by sectioning the original, beginning at the upper left-hand corner and continuing from left to right in equal sections with small overlaps.

ProQuest Information and Learning
300 North Zeeb Road, Ann Arbor, MI 48106-1346 USA
800-521-0600

Turbo Coded OFDM with a Novel Synchronization Technique for Broadband Wireless Applications

Jinglei Liu

A thesis

in

The Department

of

Electrical and Computer Engineering

Presented in Partial Fulfillment of the Requirements

For the Degree of Master of Applied Science at

Concordia University

Montreal, Quebec, Canada

August 2002

ABSTRACT

Turbo Coded OFDM with a Novel Synchronization Technique for Broadband Wireless Applications

Jinglei Liu

Broadband Wireless Access (BWA) has become the best way to meet the escalating demand for connecting people to the Internet primarily because of its flexibility and low cost. The rapid growth of wireless subscribers and their requirements of integrated data, voice and video services pose a great challenge when designing high-speed wireless systems with reasonable Quality of Service (QoS) given the limited resource of radio spectrum. In recent years, Orthogonal Frequency Division Multiplexing (OFDM) has gained a lot of attention in diverse high-speed digital communication applications. This has been due to its favorable properties such as high spectral efficiency and robustness to multipath delays.

In this thesis, an OFDM system, featuring a novel bandwidth efficient synchronization technique robust to multipath propagation, is presented and analyzed. The timing offset and frequency errors due to the transmission over a wireless multipath fading channel can result in rapid bit error rate degradation in OFDM systems. The idea of the proposed simple and efficient synchronization technique is to reduce this degradation by designing a synchronizer with a smaller error variance and also less overhead. This enables us to strengthen the robustness of OFDM to severe multipath

propagations by successfully removing the cyclic prefix (Inter Symbol Interference free) and maintaining the orthogonality between all the subcarriers (Inter Channel Interference free). Furthermore, the thesis focuses on the application of diverse channel coding for the coded orthogonal frequency division multiplexing (COFDM). The performances of the COFDM based on Turbo Convolutional code (TCC) and Turbo Block code (TBC) are analyzed and compared. This work also includes channel estimation, which is very important for coherent demodulation in OFDM.

The simulation results show that the OFDM system, with the proposed robust synchronization technique and only one properly designed training symbol. has not only better performance on both timing and frequency offset estimation, but also better bandwidth efficiency in a multipath fading channel compared with many other modified versions of the conventional methods described in the literature. The significantly small error variance of symbol timing has been reached by perfectly eliminating the plateau of timing metric in the conventional synchronization technique. Thus at low SNR there is no observable error variance of frequency offset. Furthermore, due to the high accuracy of synchronization, there is still a potential for saving more bandwidth by further shortening the guard time. In addition, the applied efficient coding scheme can give almost 10dB coding gain to the OFDM system at a bit error rate of 10^{-5} and known channel.

ACKNOWLEDGMENTS

In the first place, I would like to express my sincere appreciation and gratitude to my supervisor, Dr. Mohammad Reza Soleymani, for his criticisms, insights, thoughtful suggestions and continual prodding during the course of this study. He carefully guided me throughout the pursuit of my Master's degree at Concordia University. His ideas and suggestions have been invaluable to this thesis.

I would like to thank my examining committee Dr. Hovhannes Harutyunyan, Dr. Walaa Hamouda and Dr. Chunyan Wang for reading this text and evaluating my work.

I am grateful to Dr. Yongzhe Xie whose ideas were useful to this thesis.and Dr. Johan for his insightful suggestions and assistance at my work. The discussions with them have contributed substantially to this work. I also wish to express my sincere gratitude to my dear friends Usa and Eric for their help whenever I was in need. I extend my appreciation to many other friends and classmates at Concordia, especailly to Mohammad, Dr. Li, Behzad.

Finally, I owe special gratitude to my husband, Yi Yang, and my parents for their continuous and unconditional support.

TABLE OF CONTENTS

LIST OF FIGURES

GLOSSARY

ADC	Analog-to-Digital Conversion
ADSL	Asymmetric Digital Subscriber Line
ARC	Analysis, Research, and Consultancy group
AWGN	Additive White Gaussian Noise
BER	Bit Error Rate
COFDM	Coded Orthogonal Frequency Division Multiplexing
DAB	Digital Audio Broadcasting
DFT	Discrete Fourier Transform
DSL	Digital Subscribe Line
FDM	Frequency Division Multiplexing
FEC	Forward Error Correction
FFO	Fractional part of the Frequency Offset
FFT	Fast Fourier Transform
FO	Frequency Offset
ICI	Inter-Carrier Interference
IDFT	Inverse Discrete Fourier Transform
IFFT	Inverse Fast Fourier Transform
IFO	Integer part of Frequency Offset
ISI	Inter-Symbol Interference

MC	Multi-Carrier
ML	Maximum Likelihood
OFDM	Orthogonal Frequency Division multiplexing
PAP	Peak-to-Average Power ratio
PCCC	Parallel Concatenated Convolution Codes
RCS	Recursive Systematic Convolutional
RS	Reed-Solomon
SC	Single Carrirer
SCCC	serial concatenated convolutional codes
SNR	Signal to Noise Ratio
TBC	Turbo Block Code
TCC	Turbo Convolutional Code
TCM	Trellis-Coded Modulation
TPC	Turbo Product Code
TO	Timing Offset
WLAN	Wireless Local Area Network

Chapter 1

Introduction

In recent years, there has been a significant increase in the demand for multimedia applications due to the rapid growth of the voice, video and data communication market. These applications are evolving toward a reliable broadband communication system supporting various kinds of services as well as voice services. The swift growth for the demand of high speed Internet (World Wide Web) access and multi-line voice for residential and small business customers has created a necessity for last mile broadband access. The integration of today's access system includes both wired and wireless networks. Wireless communications has evolved from being an expensive and rare technology for limited customers in the 1970's, to becoming a widespread and economical means for facilitating domestic, commercial, as well as public service communications. Broadband wireless access is the most challenging segment of the wireless revolution given that it has to demonstrate a viable alternative to cable modem and DSL (Digital Subscribe Line) technologies, which are well-established in the last mile access environment. According to the forecast of the Analysis, Research, and Consultancy (ARC) group, the fixed wireless deployments in both homes and businesses will reach almost 28 million by 2005.

For the realization of broadband air-interfaces of a wireless access, the requirement of the data rates could be up to 155 Mbits/second and beyond. The challenge of designing a digital communication system has become how to transmit such a high rate of data through a

communication channel of limited bandwidth while still maintaining maximum data reliability. There is a complication in achieving high data rates due to the time-dispersive characteristics of the channel. The *inter-symbol interference (ISI)* is one of the most severe problems in the high-speed band-limited communications. In a typical wireless scenario there are multipath-channels (i.e. the transmitted signal arrives at the receiver using various paths of different length). Since multiple versions of the signal interfere with each other (ISI), it becomes very hard to extract the original information. The degradation due to ISI becomes more severe as the target data rate becomes high. Besides, the availability of the channel bandwidth will be even more critical because of the rapid increase in the number of communication subscribers.

1.1 Overview of OFDM

Orthogonal Frequency Division multiplexing (OFDM) has grown to be the most popular system for high-speed communications in the last decade. In fact, it has been said by many industry leaders that OFDM technology is the future of wireless communications[1][2][3]. OFDM is sometimes called multi-carrier or discrete multi-tone modulation. *Frequency Division Multiplexing (FDM)* has been used for a long time to carry more than one signal over a communication channel[25]. In older multi-channel systems using FDM, the total available bandwidth was divided into N non-overlapping frequency sub-channels. Each sub-channel was modulated with a separate symbol stream and the N sub-channels were frequency multiplexed. Even though the prevention of spectral overlapping of sub-carriers reduces (or eliminates) Inter-channel Interference, this leads to an inefficient use of spectrum. The guard band on either side of each sub-channel is a waste of precious bandwidth. To overcome the problem of bandwidth wastage, OFDM spread spectrum technique distributes the data over a

number of N overlapping subcarriers each carrying a baud rate of 1/T and spaced apart at a precise frequency of 1/T. As a result of the frequency spacing selected, the sub-carriers are all mathematically orthogonal to each other. Orthogonal in this respect means that the sub-carriers are totally independent. Thus, it prevents the demodulators from seeing frequencies other than their own.

Spectral efficiency is one of the benefits of OFDM. The orthogonality of sub-carriers, which permits the proper demodulation of the symbol streams without the requirement of non-overlapping spectra, leads to a source of spectral efficiency in OFDM. Another source of OFDM spectral efficiency is the fact that the drop-off of the signal at the band is primarily due to a single carrier, which is carrying a low data rate. OFDM allows for sharp edges that correspond closer to the desired rectangular shape of the spectral power density of the signal.

OFDM is a technology with the concept of multicarrier communications. As multicarrier communications is introduced, with the fixed bandwidth, it enables an increase in the overall capacity of communication, thereby increasing the overall throughput. With OFDM, a high throughput, which may be impossible to be implemented using single carrier systems, is achievable.

One of the main advantages of OFDM is that it leads to less intersymbol interference than if the overall throughput was attempted on a single carrier system. Data are transmitted in parallel using a number of subcarriers in the OFDM system. It is easy to observe from the concept of OFDM that for achieving the same throughput, the symbol-rate of OFDM is N times of that of single carrier system. By increasing the symbol duration and also cyclically

extending a guard time, the OFDM system convers a frequency-selective fading channel into a frequency-flat fading channel, thus, strongly acting against the intersymbol interference.

The roots of OFDM date back to the late 1950's, with the technology gaining popularity when it became the standard for Digital Audio Broadcasting (DAB). Since the late 1970's, OFDM has been proposed and adopted in standards for high-speed applications. OFDM is currently used in the European digital audio broadcasting standard and its applicability to digital TV broadcasting is currently being investigated. It also forms the basis for the global Asymmetric Digital Subscriber Line (ADSL) standards. In 1999, the IEEE 802.11 working group published IEEE802.11a, which outlines the use of OFDM in the 5.8 GHz band for Wireless Local Area Network (WLAN). The IEEE 802.16 broadband wireless access working group also adopted OFDM for air interface of the physical layer in 2002.

For an OFDM system, it can be shown that the modulation of orthogonal sub-carriers can be represented as an Inverse Fourier Transform. In order to reduce the computation complexity, a Fast Fourier Transform (FFT) and its inverse are normally employed in the design of an OFDM system. Compared with the single carrier systems, the implementation complexity of the OFDM system is largely determined by the FFT/IFFT block. The block diagram of an OFDM system is shown in Figure 1.1, where the upper path is the transmitter chain and the lower path corresponds to the receiver chain. The IFFT/FFT in the center of the figure modulates (IFFT) a block of input values onto a number of subcarriers in the transmitter and demodulates (FFT) the signal in the receiver.

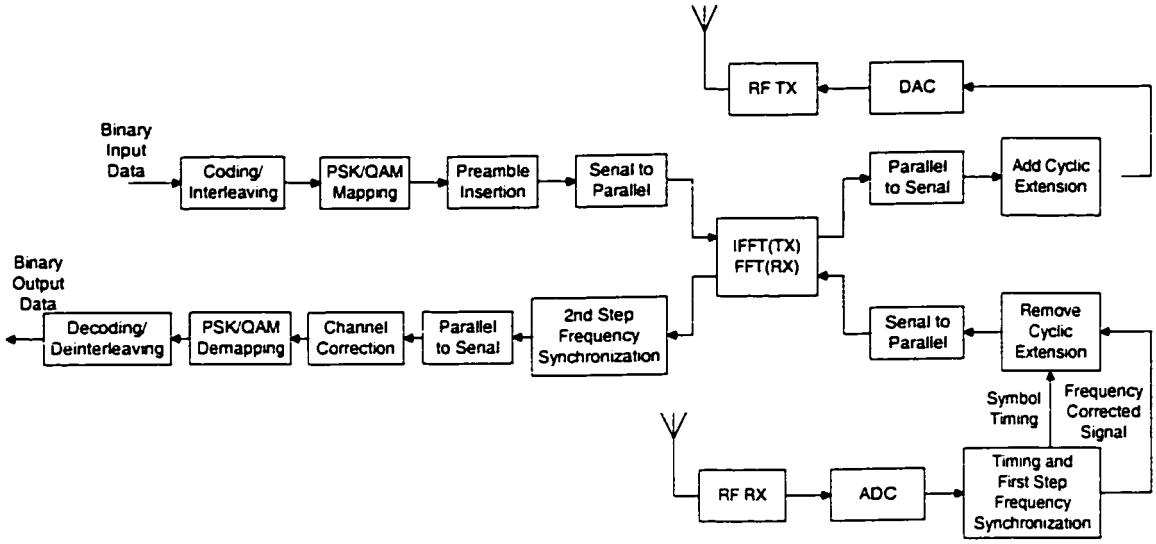

Figure 1.1 Block diagram of an OFDM transceiver

1.2 Coded OFDM

It is uncommon to use uncoded OFDM as shown in Figure 1.1. In fact, almost all current OFDM implementations use Forward Error Correction (FEC). First of all, the OFDM technique is one of multi-amplitude and frequency modulation. Therefore, the OFDM signal is contaminated by nonlinear distortion of the transmitter High-Power Amplifier. Channel coding becomes a commonplace compensation technique. Additionally, many independent subcarrier signals cause large amplitude variation in the received OFDM signal. By using coding, the subcarriers in deep fades are to be corrected somehow so that the system performance is determined by average received power rather than the lowest subcarrier powers. Therefore, FEC makes OFDM more effective and reliable.

Today, there are many FEC schemes available, either accepted in the current popular wireless communication system, or under development in the OFDM research community. For instance, Convolutional codes are one of the mostly widely used channel codes in today's

systems; all the major cellular systems (GSM, IS-95) in use today use convolutional channel codes. IEEE 802.11a and HiperLAN/2 WLAN standards also use convolutional error correcting codes. As for IEEE 802.16a, it includes an optional mode that uses them. Moreover, Reed-Solomon (RS) block codes used for Intelsat, Digital Video Broadcasting (DVB) concatenated with convolutional Viterbi codes offer an improvement over stand-alone Reed-Solomon (RS) block codes, and they are one of the optional coding schemes included in the IEEE 802.16a standards. Finally, the Turbo Convolutional Code (TCC) scheme resembles the Turbo Codes used in 3GPP (W-CDMA) and 3GPP2 (CDMA2000) as well as Digital Video Broadcasting Return Channel over Satellite (DVB-RCS). Though unlike Turbo Product Codes (TPC) it has not been chosen as the coding scheme for IEEE 802.16, but the relevant study on it for COFDM in IEEE 802.11a can be found in [1]. A general comparison of TCC and TPC in OFDM system will be carried out in detail.

1.3 Estimators of OFDM system

OFDM is a solution for high-speed data transmission with multipath immunity. As shown Figure 1.1, by using the IFFT, serial high-speed signals will be modulated to many orthogonal subcarriers and then transmitted in parallel. The orthogonality between subcarriers is ensured by an extended symbol duration of each subcarrier plus the cyclically extended guard interval. Thus, the ISI and ICI due to multipath delay could be perfectly avoided. However, this will only be true under the assumption that the receiver is perfectly synchronized to the transmitter.

As a matter of fact, the orthogonality is easily destroyed by the synchronization issues in the transmission of OFDM. First, any frequency offset instantly causes amplitude fading and the ICI. Consequently, OFDM is particularly sensitive to it more than single carrier systems. A symbol timing offset gives rise to a phase rotation of the subcarriers however, by using a cyclic prefix the timing requirements are relaxed somewhat. If a timing error could be suppressed small enough to keep the channel impulse response within the cyclic prefix, the orthogonality will be maintained.

A great deal of attention is given to both symbol and frequency synchronization in OFDM systems. Some of the common methods used to achieve synchronization in OFDM systems are synchronization using cyclic extension and synchronization using training sequence in the presence of multipath. The synchronization algorithm based on training sequence is usually simple and efficient for packet oriented applications defined in many of the previously mentioned broadband system standards. Further, the channel impairments must be recovered by channel estimation schemes if coherent demodulation was employed.

1.4 Motivation

One of the disadvantages of OFDM system is that it is very sensitive to synchronization issues, especially frequency offset, which can easily destroy the orthogonatlity between OFDM subcarriers. Usually, the two main tasks of synchronization are to estimate the symbol timing and frequency offset.

In previous literature[6][7][8][9][10], many different timing and frequency estimators were proposed. They can be divided into two main groups: estimators based on cyclic prefix

and preamble (training symbols). Estimators using cyclic prefix as guard time interval are mainly used for continuous transmission such as broadcasting applications. The estimator using training symbols is preferred in packet oriented burst transmission. Therefore, in our newly proposed synchronization technique, the one based on training symbols is chosen.

Four typical synchronization techniques based on training symbols were proposed earlier. In [7]-[10], one or two training symbols (pilot tones) were used for both or either one of the symbol timing and frequency offset estimations. In [8], Schmidl and Cox improved the P. Moose estimator [7], and introduced a conventional synchronization method using two training symbols. However, their scheme has four drawbacks: a) low bandwidth efficiency due to need for two training symbols, b) their estimator cannot get accurate symbol timing by eliminating the plateau of their timing metric, c) the need for further computation to detect exact value of timing offset (because of the timing metric plateau) increases the computational complexity even more, d) the inaccurate estimation in timing also directly leads to the imprecise frequency offset estimation at low SNR. In [9], the authors modified the method to find the integral part of the frequency offset in order to increase the bandwidth efficiency by using one training symbol to do both estimations. In addition, an improvement on their frequency estimation at low SNR was obtained. But since they utilize the same timing estimator as [8], their intended improvement is quite limited. Finally, in [10], a new simple and efficient timing scheme was proposed, but their training symbol can only be used for the timing estimation. Additional training symbols must be used in order to obtain the frequency offset, so it is not a bandwidth efficient solution. In summary, the modified estimators in [9]

and [10] give a different sort of improvement, but the trade-off between bandwidth efficiency and estimator accuracy is inherent.

Therefore, the purpose of this study is to develop a simple and efficient synchronization algorithm that saves not only more bandwidth, but also gives more accuracy on both symbol timing and carrier frequency offset estimations. Moreover, in order to verify its performance comprehensively in a complete wireless communication system, the baseband model of the whole OFDM system in Figure 1.1 was established by computer simulation.

1.5 Scope and Organization of the Thesis

In this thesis, the overall system of Coded Orthogonal Frequency Division Multiplexing for packet-oriented transmission is analyzed and the performance of the system is evaluated. Because of the importance of synchronization for the robustness of OFDM in a multipath channel, more effort is placed on the design of timing and the frequency offset synchronizer for the OFDM system with the smallest possible error variance. As a result, a novel and robust timing and frequency offset estimation algorithm with more bandwidth efficiency and the best accuracy is proposed. Based on some of the existing estimation theorems, a unique modified estimation algorithm is also presented. Its great improvement on the estimator performance is only surpassed by the novel and robust one verified. In addition, channel estimation is applied to conquer the channel distortion, and two powerful channel coding scheme, TCC and TPC, are also comparatively studied so as to enhance the overall system performance in a multipath fading channel.

The thesis is organized in the following approach. In Chapter 2, some background materials on the principle of the OFDM systems are presented. In Chapter 3, two new training symbol based synchronization techniques for OFDM systems are proposed and studied comparatively with several other similar research works concerning their bandwidth efficiency and accuracy. In Chapter 4, a simple channel estimator for the coherent demodulation of the OFDM system is given. In Chapter 5, an overall performance for a whole system of COFDM with synchronizer and channel estimator are discussed. Finally in Chapter 6, the results of this investigation are summarized, the contribution highlighted, and the direction for some further study suggested.

Chapter 2

Background

In a multipath channel, most conventional modulation techniques are sensitive to intersymbol interference unless the channel symbol rate is small compared to the delay spread of the channel. However, OFDM, a multi-carrier modulation technique with densely spaced sub-carriers, is less sensitive to the delay spread and also provides high symbol rate. Therefore, it has gained a lot of popularity among the broadband community in the last few years. The basic idea of OFDM systems, its mathematic background and advantages and disadvantages are briefly presented in this Chapter.

2.1 OFDM System Model

The principle motivation of employing OFDM is to use parallel data and frequency division multiplexing with orthogonal overlapping subchannels to avoid the use of high-speed equalization and to combat multipath delay spread as well as to fully use the available bandwidth. Due to the implementation problems of large number of carriers at the transmitter, the system implementation was delayed for nearly 20-25 years. The recent development in DSP and VLSI technologies make OFDM a feasible technique today.

2.1.1 Basic OFDM signal

In the most general form, the equivalent complex baseband OFDM signal can be written as a set of modulated carriers transmitted in parallel, as follows:

$$x(t) = \sum_{n=-\infty}^{\infty}\left(\sum_{k=0}^{N-1} X_{n,k}\, g_k(t - nT_s)\right) = \sum_{n=-\infty}^{\infty} x_n(t) \tag{2.1}$$

$$g_k(t) = \begin{cases} e^{j2\pi f_k t} & t \in [0, T_s) \\ 0 & otherwise \end{cases} \tag{2.2}$$

$$f_k = \frac{k}{NT_s} \tag{2.3}$$

where T_s represents the symbol interval of the original symbols. $X_{n,k}$ is the symbol (complex numbers from a set of signal constellation points) transmitted on the kth subcarrier in the nth signaling interval, each of duration T_s; N is the number of OFDM subcarriers; f_k is the kth subcarrier frequency. The $x_n(t)$ is the transmitted baseband signal for OFDM symbol number n.

Demodulation is based on the orthogonality of the carriers $g_k(t)$, namely,

$$\int_{\mathbb{R}} g_k(t)\, g_l^*(t)\, dt = T_s \cdot \delta(k - l) \tag{2.4}$$

Thus the Demodulator will implement the relation:

$$X_{n,k} = \frac{1}{T_s} \cdot \int_{nT_s}^{(n+1)T_s} x(t)\, g_k^*(t)\, dt \tag{2.5}$$

Figure 2.1 shows the general structure of an orthogonal multicarrier system.

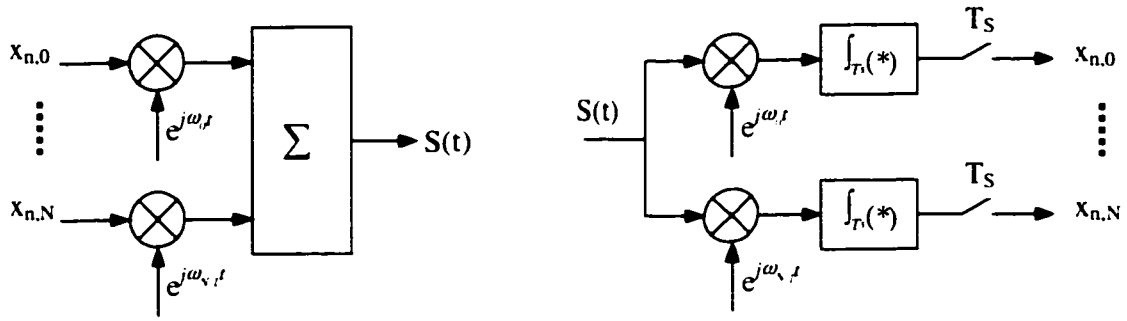

Figure 2.1 Basic Structure of an Orthogonal Multicarrier system

The property accounting for orthogonality of the different OFDM subcarriers could be demonstrated in both time and frequency domain. As explained in [3], in time domain, the orthogonality between the subcarriers is maintained as long as each subcarrier always have an integer number of cycles within the DFT integration interval. An example of three orthogonal subcarriers within one OFDM symbol is shown in Figure 2.2. Furthermore, a spectrum of individual subcarriers depicts the orthogonatlity of OFDM subcarriers in frequency domain in Figure 2.3. Having the zero crossings of all the other subcarriers at the maximum of each subcarrier spectrum, which means subcarriers in one OFDM symbol are orthogonal to each other, the intercarrier interference (ICI) can be avoided. It is so called ICI free for frequency overlapped OFDM systems.

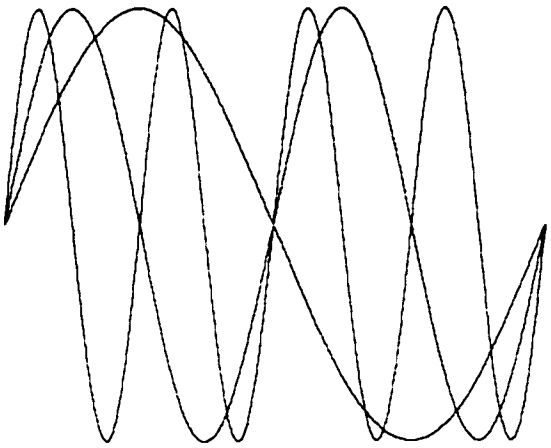

Figure 2.2 Example of three subcarriers with one OFDM symbol

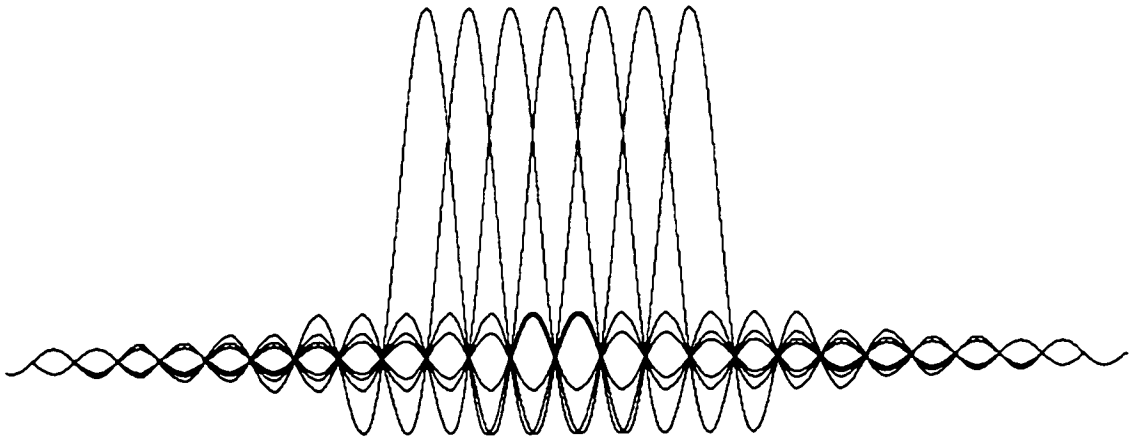

Figure 2.3 Spectra of individual subcarriers

The complex baseband OFDM signals defined by (2.1) are generated by the basic orthogonal multicarrier modulator with large number of sub modulators for each orthogonal subcarrier. In practical, that kind of system was almost not possible to be implemented. However, in (2.1) an Inverse Fourier transform can be replaced as an OFDM modulator alternatively. Further, the discrete time version of (2.1) shall be

$$x_n(m) = \sum_{k=0}^{N-1} X_{n,k}\, g_k(t - nT_s)\Big|_{t=(n+\frac{m}{N})T_s}, m = 0...N-1 \tag{2.6}$$

$$x_n(m) = \left(\sum_{k=0}^{N-1} X_{n,k} e^{j2\pi k\frac{m}{N}}\right) = \sqrt{N} \cdot IDFT\{X_{n,k}\} \tag{2.7}$$

From (2.7), the OFDM modulation is nothing but an *Inverse Discrete Fourier transform* can *(IDFT)*, as shown in Figure 2.4(a) where P/S and S/P stands for parallel to serial and serial to parallel converter. The use of *Discrete Fourier Transform (DFT)* in the parallel transmission of data using Frequency Division Multiplexing has already been investigated since 1971. Though IDFT algorithm dramatically simplified the OFDM multicarrier modulator, it is still not efficient enough when number of carrier is more than 32 due to the computation complexity of this direct form of DFT. Fortunately a series of "fast" transforms have been developed that are mathematically equivalent to the DFT, but which require significantly fewer computer operations for their implementation. It is so called *Fast Fourier Transform* (*FFT*). The concept and analysis of FFT and IFFT can be found in [5]. IFFT, Corresponding to IDFT, then is chosen to be the multicarrier modulator in OFDM system, as shown in Figure 2.4 (b). The Demodulator basically does the reverse operation to the modulator, so the OFDM demodulator just does the FFT, as shown in Figure 2.5.

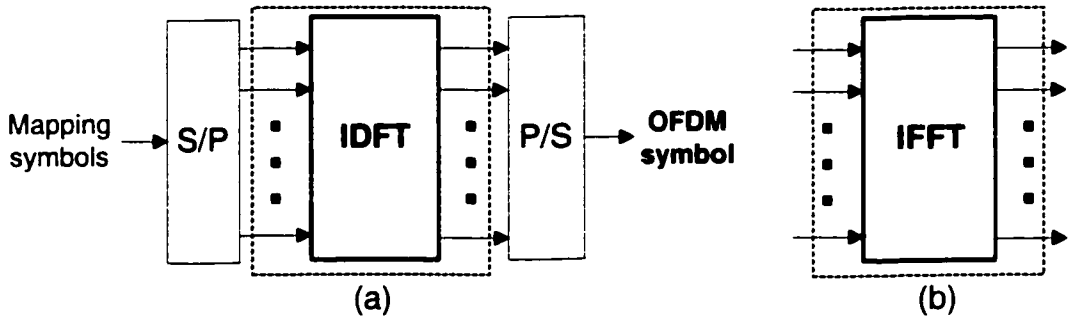

Figure 2.4 OFDM Modulator

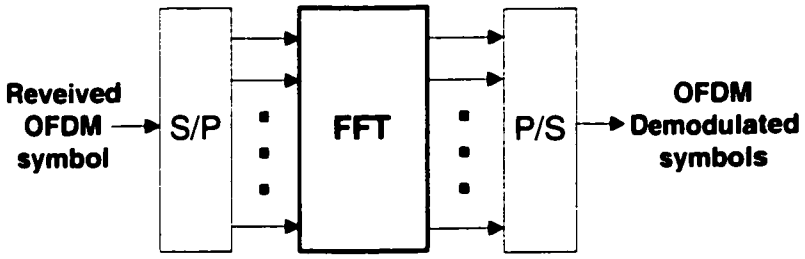

Figure 2.5 OFDM Demodulator

2.1.2 Introduction of Guard Period and Cyclic Prefix

One of the main advantages of OFDM is its effectiveness against the multi-path delay spread frequently encountered in wireless communication channels. The reduction of the symbol rate by N times, results in a proportional reduction of the relative multi-path delay spread, relative to the symbol time. To completely eliminate even the very small ISI that results, as shown in Figure 2.6(a), a guard time is introduced for each OFDM symbol in Figure 2.6(b). The guard time must be chosen to be larger than the expected delay spread, such that multi-path components from one symbol cannot interfere with the next symbol. If the guard time is left empty, this may lead to *inter-carrier interference (ICI)*, since the carriers are no longer orthogonal to each other. To avoid such a cross talk between sub-carriers, the OFDM symbol is cyclically extended in the guard time. This ensures that the delayed replicas of the OFDM

symbols always have an integer number of cycles within the FFT interval as long as the multi-path delay spread is less than the guard time.

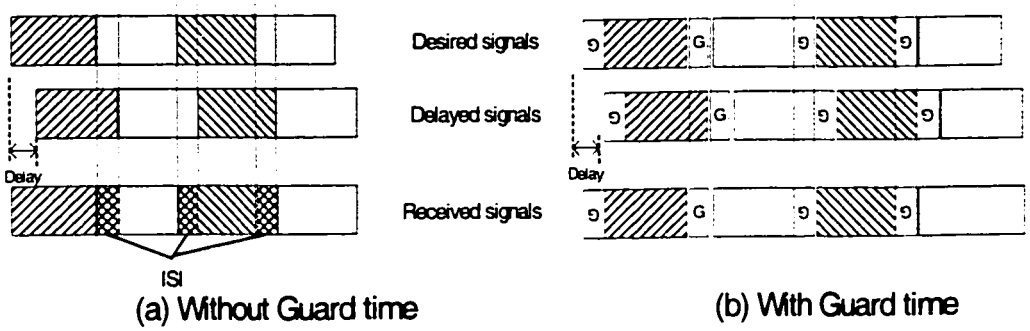

Figure 2.6 Guard period for eliminating ISI due to multipath

2.1.3 Subcarrier Mapping

Usually, BPSK, QPSK, 16-QAM, 64-QAM modulation shall be used to map the subcarrier to Gray coded constellation, illustrated in Figure 2.7, where b_0 is the earliest input bit. In order to achieve the average power for all mappings, based on the modulation mode, the output of the mapping need to be normalized by factor K_{MOD} as listed in Table 2.1.

Mapping	K_{MOD}
BPSK	1
QPSK	$1/\sqrt{2}$
16-QAM	$1/\sqrt{10}$
64-QAM	$1/\sqrt{42}$

Table 2.1 Normalized factor K_{MOD}

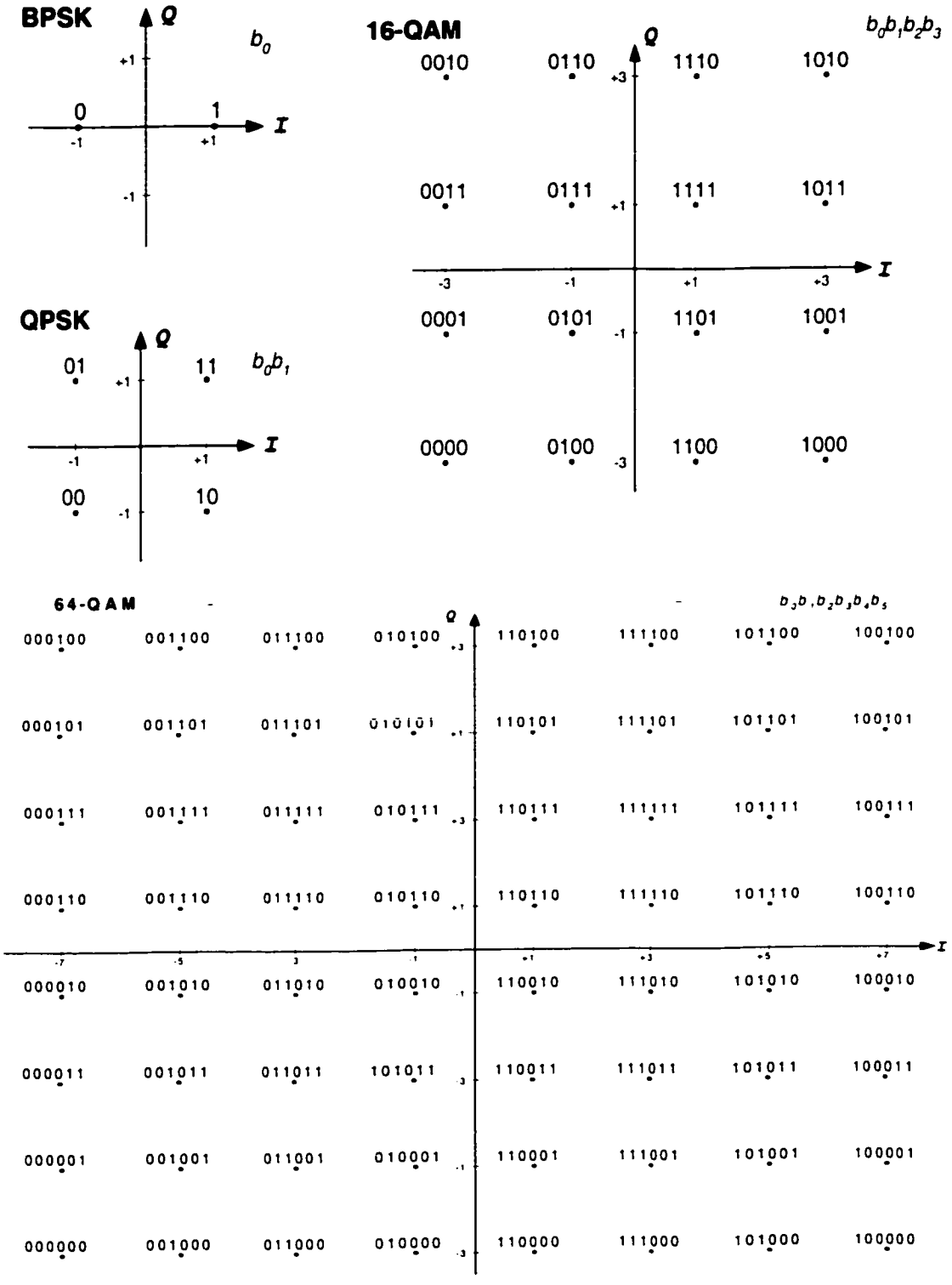

Figure 2.7 BPSK, QPSK, 16-QAM, 64-QAM mapping

2.1.4 Multipath Fading Channel

In the multipath transmission environment, shown in Figure 2.8, signal follows several propagation paths to arrive at the receiver, so there will be multiple copies of signal with different delay spread. As a result, the received signal at the receiver is corrupted in a variety of ways by frequency and phase distortion, inter symbol interference and thermal noise.

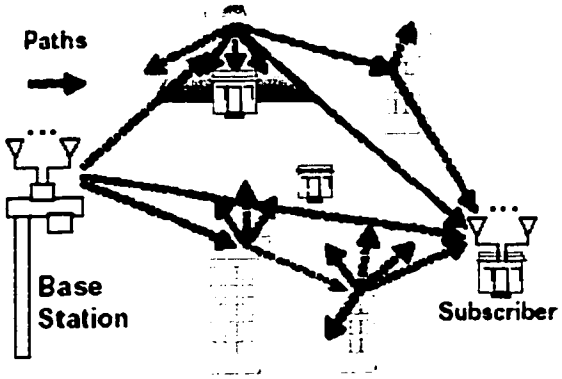

Figure 2.8 Multipath transmission environment

2.1.5 Basic OFDM system model

Based on the previous discussion, Figure 2.9 shows the basic baseband OFDM system block diagram. The random data generator generates '0' and '1' binary bits randomly. Then, the information binary bits will be fed into the subcarrier modulator to map information bits to symbols in a certain constellation according to different modulation technique used. These symbols will be converted from serial sequence into parallel form in order to parallel modulate each subcarrier using IFFT. OFDM symbols are generated at the output of IFFT multicarrier modulator, and followed by a parallel to serial converter OFDM symbols will be cyclically extended. After complex OFDM baseband symbols are sent through channel, at receiver,

things are just reversed. Cyclic prefix has to be removed first at the receiver. After the FFT multicarrier demodulator and demapping, the recovered binary information bits will be serially output.

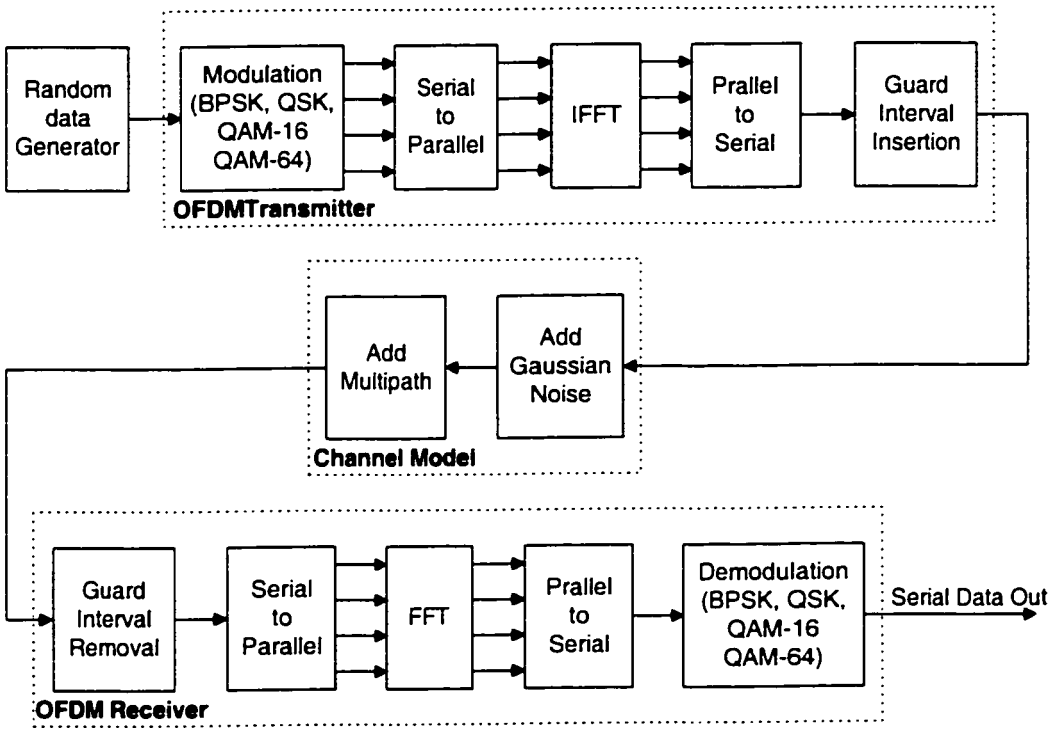

Figure 2.9 Basic OFDM system model

Under these assumptions,

1. The channel being considered time-invariant during the transmission of one OFDM symbol, and the impulse response of the channel is shorter than the cyclic prefix.

2. ISI is avoided by perfect removal of the guard interval at the receiver, which requires good knowledge of the starting point of the effective (FFT) period of the OFDM symbol.

3. Perfect frequency synchronization at the OFDM receiver is necessary to avoid inter-channel-interference (ICI).

The OFDM system in Figure 2.9 can be modeled as a simple set of Gaussian channels as depicted in Figure 2.10. The $\{x_k\}$ stand for the transmitted signals at each sub-carrier, being characterized by the used modulation method. The influence of the fading radio channel is expressed by $\{ H_k \}$, the complex-valued frequency response of the multipath fading channel; additive white Gaussian noise (AWGN) is denoted as $\{ w_k \}$. $\{ r_k \}$ are the received signals .

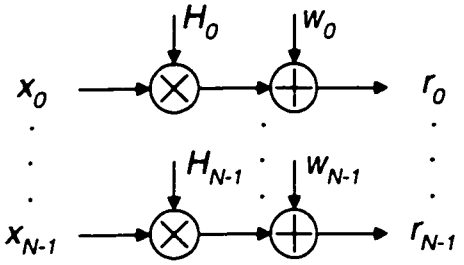

Figure 2.10 Simple OFDM system model

2.2 Advantages and Disadvantages of OFDM

OFDM possesses some inherent advantages for Wireless Communications so that it is becoming more popular in the Wireless Industry today. Due to the symbol duration on the subcarriers is increased relative to delay spread and the use of guard interval, ISI is avoided and OFDM is more tolerant of delay spread than single carrier systems. Hence, the most important advantage of OFDM is its Robustness in multipath propagation environment.

OFDM provides higher data rate but with simplified equalization as compared to single carrier systems. That means it gives better performance with less complexity. With

coding technique, COFDM is more resistant to multipath fading for FEC is powerful to protect OFDM subcarriers from suffering a deep fade. Even though, OFDM provides a lot advantages for Wireless Transmission, it has a few serious disadvantages that must be overcome for this technology to become a success.

One of the most serious problems with OFDM transmission is that, it exhibits a high peak-to-average power ratio (PAP). PAR can be solved in many ways and detailed studies on it can be found in [4] if interested.

Another important issue in OFDM transmission is synchronization. There are basically two issues that must be addressed in synchronization.

1. The receiver has to estimate the timing so as to minimize the effects of inter-carrier interference (ICI) and inter-symbol interference (ISI).

2. In an OFDM system, the sub-carriers are exactly orthogonal only if the transmitter and the receiver use exactly the same frequencies. Thus receiver has to estimate and correct for the carrier frequency offset of the received signal.

Besides, the phase information must be recovered if coherent demodulation is employed. In the following chapters, the above mentioned disadvantages except for PAP ratio will be studied in more detail.

2.3 Summary

Multi-Carrier Modulation is a technique for data-transmission achieved by dividing a high bit-rate data stream into several parallel low bit-rate data streams and using these low bit-rate data streams to modulate several carriers. OFDM is a multi-Carrier modulation system employing Frequency Division Multiplexing (FDM) of orthogonal sub-carriers, each of which modulates a low bit-rate digital stream. OFDM Transmission has a lot of useful properties such as delay-spread tolerance and spectrum efficiency that encourage its use in many standards of wireless communications. Based on the fundamental mathematic backgrounds of OFDM modulation and demodulation, its merits and demerits have been introduced in this chapter. Some specific issues such as synchronization and channel estimation will be analyzed and investigated in the following chapter.

Chapter 3

Synchronization

In this chapter, the basic synchronization issues, one of the major disadvantages of OFDM, is analyzed first. Current available synchronization algorithms are then classified and briefly compared. Based on the aim of designing a good timing and frequency-offset estimator with more bandwidth efficiency and accuracy, two schemes are proposed and also compared with the other existing synchronization techniques in literatures.

3.1 Synchronization Issues

The OFDM is a method that allows transmitting high data rates over extremely hostile channels at a comparatively low complexity. First, the introduction of cyclic prefix as guard time eliminates both inter-symbol interference (ISI) and inter-channel interference (ICI) in the OFDM system. Second, OFDM has the advantage of spreading out a fade over many symbols, thereby reducing the sensitivity of the system to delay spread. On the other hand, one of the disadvantages of OFDM system is that it is very sensitive to synchronization issues such as timing offset and especially frequency offset. Usually, the two main tasks of synchronization are to estimate the symbol timing and the frequency offset.

3.1.1 Effects of frequency offset

Frequency offset is frequency difference between transmitter and receiver. It is created by difference in oscillators in transmitter and receiver, so called phase noise. There are two

impaired effects caused by frequency offset. One is power loss due to amplitude reduction for not peak sampling; the other is the ICI introduction since the orthogonality of subcarriers is destroyed. Figure 3.1 shows the effects.

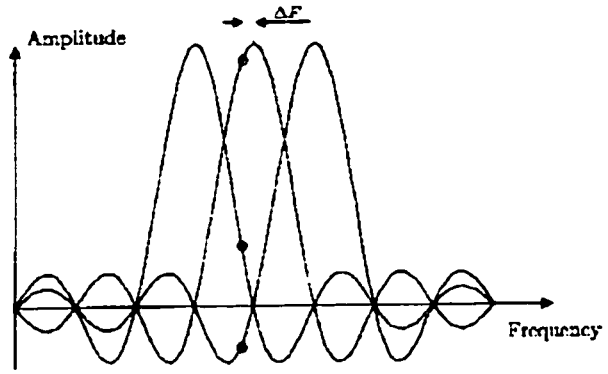

Figure 3.1 Effects of a frequency offset: reduction in signal amplitude(o) and ICI(•)

3.1.2 Effects of timing offset

In multipath channels the timing offset increases the sensitivity of OFDM to delay spread. However, By using cyclic prefix, as long as a symbol timing delay is in the loose range of guard time interval as illustrated in Figure 3.2, it can be viewed as a phase shift introduced by the channel, and this phase rotation can be estimated by a channel estimator. So, In this case, the timing offset will not introduce any ISI and ICI. Otherwise, ISI will occur. However, to achieve the best robustness to multipath propagation, there is optimal timing offset requirement [6][3].

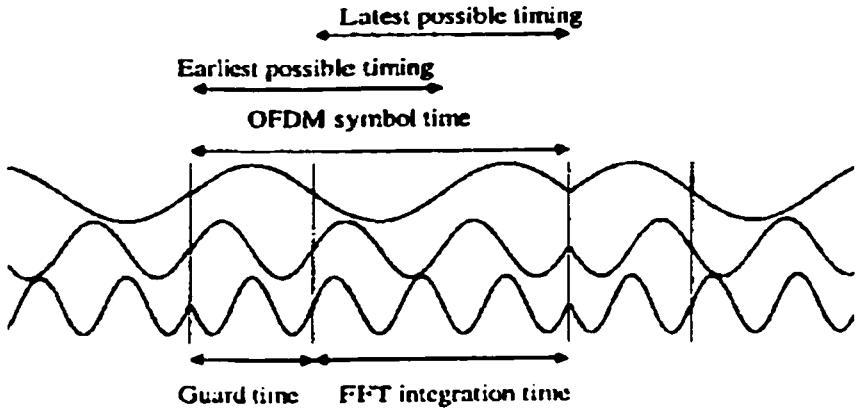

Figure 3.2 Example showing that Timing offset will not introduce ISI and ICI, no matter the earliest timing or the latest timing

3.2 System Description

A baseband OFDM signal is generated by taking the IDFT/IFFT of a block of transmitted data symbol $\{X_k\}$ belonging to a QAM or PSK constellation. We can express samples of discrete-time OFDM symbol as

$$x_n = IDFT_N\{X_k\} = \frac{1}{\sqrt{N}} \sum_{k=0}^{N-1} X_k e^{j\frac{2\pi nk}{N}} \tag{3.1}$$

where $-G \leq n \leq N-1$, N is the IDFT/IFFT size, G is the number of cyclic prefix samples which is served as guard time to conquer multipath channel and must be greater or equal to the time spread of the channel to avoid ICI and ISI, and the sampling rate is $1/T_s = N/T$ ($1/T$ is subcarrier spacing). Furthermore, due to the use of IDFT/IFFT, sometimes in literatures it is clear to define $\{X_k\}$ as frequency domain signal, $\{x_n\}$ as time domain signal.

In practice, we must consider to pass our signal through a channel. A time-variant discrete-time multipath channel is characterized by

$$h(n,n) = \sum_{l=0}^{M-1} h_l(n)\delta(n_\tau - n_l) \tag{3.2}$$

where $n_\tau = \tau/T_s$, $\{n_l = \tau_l/T_s\}$ is the time delays normalized to T_s, $\{h_l(n)\}$ represents the complex path gains of lth path, and M is the total number of the paths. If the carrier *frequency offset* (FO) Δf and the normalized *symbol timing offset (TO)* $\varepsilon_0 = \tau_0/T_s$ caused by timing estimator affect our received signal, the channel output signal after passing through the multipath fading channel is in the form of

$$r_n = \sum_{l=0}^{M-1} h_l(n+\varepsilon_0)x_{n+\varepsilon_0-n_l}e^{j2\pi\Delta f(n+\varepsilon_0)} + w_{n+\varepsilon_0} \tag{3.3}$$

If ε_0 belongs to $\{-G+\tau_{max}/Ts, -G+\tau_{max}/Ts+1,\ldots,0\}$, the received signal is ISI and ICI free, where τ_{max} is the maximum multipath delay spread. That means, there is optimal timing offset requirement. On the contrary, if ε_0 is out of this range, both ISI and ICI will be introduced as shown in Figure 3.3. The extra ISI+ICI term will cause major performance degradation. In order to eliminate this and also shorten the guard time interval as much as possible, we need to design an estimator such that the timing error is small compared to the required timing offset interval. Otherwise, if the longer cyclic prefix is used to ensure that the timing offset within the ISI free region, it will reduce the bandwidth efficiency.

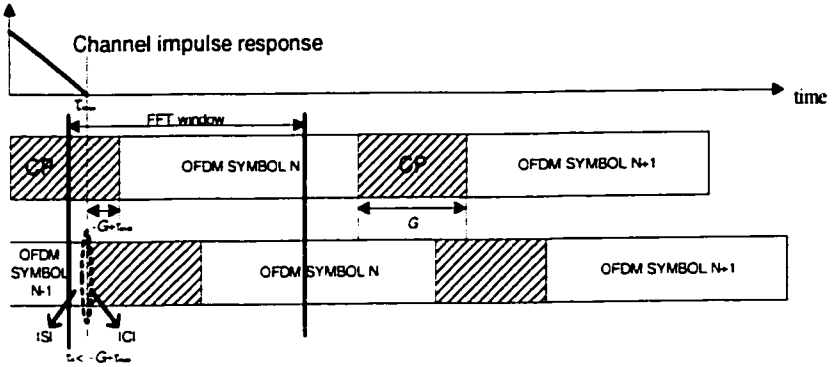

Figure 3.3 Non-optimum timing offset leads to ISI+ICI.

Let us assume that ε_0 is in the range $\{-G+\tau_{max}/Ts \ldots 0\}$ and the channel is time-invariant $h_l(n+\varepsilon_0) = h_l$ in one OFDM symbol. After substituting (3.1) with $n = n+\varepsilon_0-n_l$ into (3.3), the sampled complex envelope of the received sequence is given by

$$r_n = \frac{e^{j\theta_0}}{\sqrt{N}} \sum_{k=0}^{N-1} H_k e^{j\frac{2\pi k\varepsilon_0}{N}} X_k e^{j\frac{2\pi n(k+\nu)}{N}} + w_{n+\varepsilon_0} \tag{3.4}$$

where $\theta_0 = 2\pi\Delta f\varepsilon_0$, $H_k = \sum_{l=0}^{M-1} h_l e^{-j2\pi k n_l / N}$, ε_0 is the normalized timing offset, $\nu = \Delta f N$ is the normalized carrier frequency offset, and $w_{n+\varepsilon_0}$ is the samples of Additive White Gaussian Noise(AWGN). From(3.4), we notice that the effect of timing offset and frequency offset on the received OFDM signal is to destroy the orthogonality between the subcarriers and to cause attenuation. Therefore, it degrades the system performance severely. Both frequency offset and timing offset should be estimated accurately and compensated.

3.3 Synchronization Algorithm

Two types of synchronization algorithm based on the cyclic extension and special training symbols are commonly used for OFDM systems. The Synchronization technique based on the cyclic extension is basically used for blind synchronization where it is not possible to use a training sequence. However, to attain a distinct correlation peak, a large (>10) number of OFDM symbols are needed, while only a fraction of each symbol is used. Such a high cost for synchronization accuracy is not affordable for the high rate packet oriented transmission. By contrast, synchronization based on the training symbols takes shorter synchronization time without losing the accuracy, so it is more efficient choice concerning to packet transmission.

In [8], Schmidl and Cox improve the P. Moose estimator [7], and propose their conventional estimator for both the timing and frequency offset using two different and properly designed training symbols. Unfortunately, their symbol timing (the start point of FFT window) cannot be uniquely found due to the timing metric plateau in the interval of cyclic prefix (see Figure 3.7). In addition, their frequency offset estimator gives the large error variance in multipath fading channel at SNR less than 10dB. In [9], authors modify a part of Schmidl and Cox method to find the frequency offset more accurately. Meanwhile, they also improve the bandwidth efficiency. However, they use the same timing estimator of Schmidt and Cox. Therefore, due to the inaccurate symbol timing, their modified frequency offset estimator can still not handle the large error variance at SNR lower than 5dB(see Figure 3.12). In [10], authors redesign the Schmidl and Cox's training symbol and get the high accuracy of timing offset estimation. On the other hand, their redesigned training symbol is only designed to cope with symbol timing, and it is not suitable for frequency estimation. If the frequency

offset is also to be estimated, at least one other training symbol is needed. In summary, a tradeoff between high synchronization accuracy and the bandwidth efficiency exists in all above-mentioned algorithms.

Using only one training symbol, the two synchronization schemes proposed next can estimate both the symbol timing and the frequency offset with high accuracy. In order to accomplish the synchronization tasks, some modification need to be made on the receive side. Figure 3.4 depicts the developed baseband OFDM system model considered in this chapter for the two schemes. At the receiver, in order to remove guard time, symbol timing is first estimated. It will be shown later that the FO estimation is realized in two steps. Before the FFT, the fractional part of the frequency offset (FFO) has to be estimated and corrected and then the integer part (IFO).

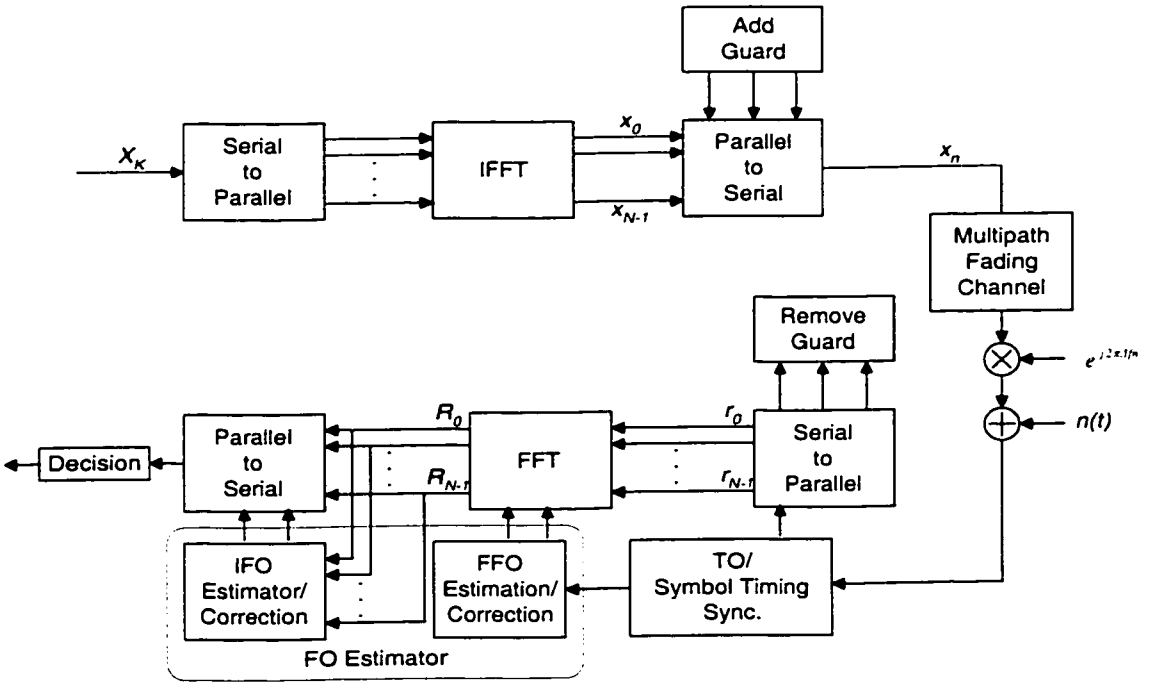

Figure 3.4 Developed baseband OFDM system model.

3.3.1 Scheme one

With a new designed training symbol, the symbol timing can be obtained as simply and precisely as in [10]. In addition, the frequency offset can also be estimated more precise than the one in [8][9].

3.3.1.1 Timing Detection

In [10], two OFDM symbols are used as training symbols for timing and frequency offset estimations. The main part of the one training symbol for the symbol timing is in the form of two repeated parts. Since the two sequences with the length of N/2 are repeated to each other, at the receiver the symbol timing is found by maximizing a correlation metric generated by slicing a length N correlation window on the received signals. However, because the CP is cyclically extended in the training symbol, the correlation metrics calculated within the CP are the same. Due to this plateau it is impossible to find the single timing peak. Their solution is to find the approximate peak by averaging two points with 90% value of the maximum correlation metric, but such increased complexity does not reward more accuracy. Based on Schmidl&cox's method, [10] found a better solution to eliminate the plateau by a redesigned training symbol as shown in Figure 3.6(a). Because of the introduction of some negative values to the correlation metric calculated within CP, the correlation metric plateau disappeared. Instead of the training symbol design method described in [10], our new designed training symbol adds the cyclic prefix just simply by a negative copy of a tail portion of the main part of the training symbol. Because the negative samples in the cyclic prefix are able to give enough negative value in timing correlation metric over the whole cyclic prefix interval (see Figure 3.6(b)), we can also eliminate the timing metric plateau in Schmidl&cox's method

and get the perfect peak in timing metric $M_1(d)$. The frame structure of OFDM signals with designed training symbol is shown in Figure 3.5.

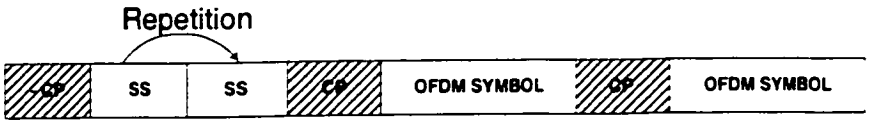

Figure 3.5 Frame structure of OFDM system.

The proposed new design training symbol $x_{0,n}$ in the time domain is designed as

$$x_{0,n} = [-CP \;\; SS \;\; SS] \tag{3.5}$$

where [*SS SS*], which is the main part of the training symbol, represents two identical sample sequences of length $L=N/2$ generated by transmitting PN sequence $\{X_k\}$ in the frequency domain on the even subcarriers, while zeros on the odd subcarriers of OFDM modulator. An illustration of a sequence belonging to QPSK constellation which can generate the main part ($N=8$-point FFT) of the training symbol in (3.5) is shown in Table 3.1.

Subcarrier #	*PN sequence* X_k	$D_k = \frac{X_k}{X_{k+2}}$
0	$(1+j)$	-j
1	0	
2	$(1+j)$	-j
3	0	
4	$(1+j)$	1
5	0	
6	$(1+j)$	1
7	0	

Table 3.1 Example of sequence to generate the training symbol

The timing metric is also calculated as

$$M_1(d) = \frac{|P_1(d)|^2}{R_1^2(d)} \tag{3.6}$$

where $P_1(d)$ is the simple correlation of two identical parts of the training symbol.

$$P_1(d) = \sum_{m=0}^{L-1} (r_{d+m}^{*} \cdot r_{d+m+L}) \tag{3.7}$$

compared with correlation calculation among four identical parts in Figure 3.6 (a), this represents a reduction in complexity as shown in Figure 3.6 (b). The half symbol energy $R_1(d)$ is calculated as half of the full N sample energy which is much better to be used according to [10],

$$R_1(d) = \frac{1}{2}\sum_{m=0}^{N-1} |r(d+m)|^2 \tag{3.8}$$

$P_1(d)$ and $R_1(d)$ can be calculated iteratively [10]. The sample index $\hat{d} = d_{max}$ which maximizes (3.6), will be the start point of the FFT.

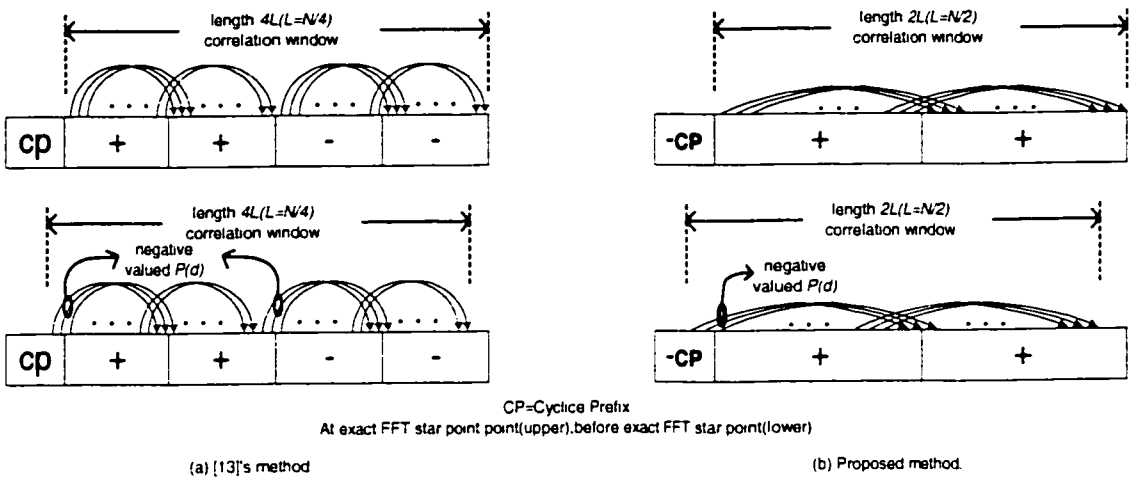

Figure 3.6 The correlation calculation comparison

An example of properly designed training symbol with 16-point FFT samples plus two samples of cyclic prefix is used to verify and compare the proposed algorithm with those of others. Without adding Gaussain noise and multipath channel, Figure 3.7 shows that the proposed method can find the desired timing metric peak at $d_{max}=21$ as perfect as in [10].

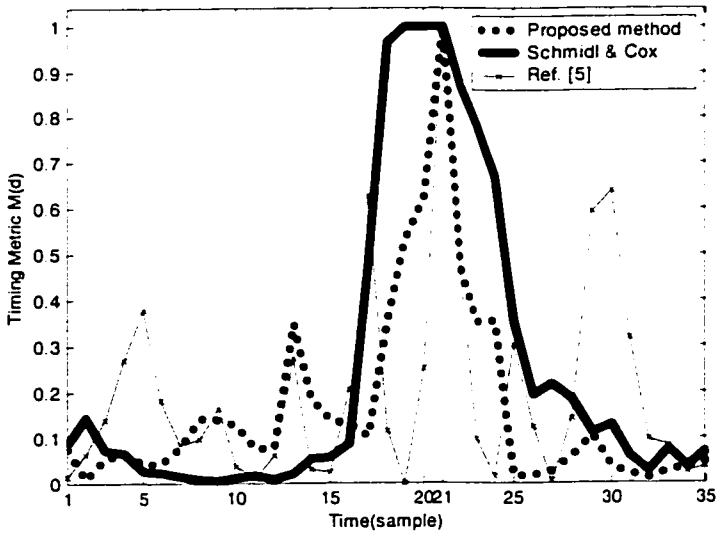

Figure 3.7 Timing metric comparison (without white noise and attenuation)

The above mentioned timing estimation method will be efficient enough in AWGN channel. However, in a Multipath channel, it has an inherent problem because the correlation is based on two repeated parts in one training symbol but not on a known training symbol. As shown in Figure, the difference of the received signals at $t=t_a$ and $t=t_a+NT_s$ will lead to weak correlation so that cause a major performance degradation. However, toward the end of the correlation calculation this kind of detrimental becomes smaller since the two received signals at $t=t_b$ and $t=t_b+NT_s$ are identical. In order to solve this unequally weighted correlation, a linear weighting function $W(m)=a_w \cdot m$ is employed, where a_w is a factor indicating the slop of the weighting function curve. As shown in next section, with the increasing a_w from 0 to 0.8, the error variance of both timing and frequency offset have been improved.

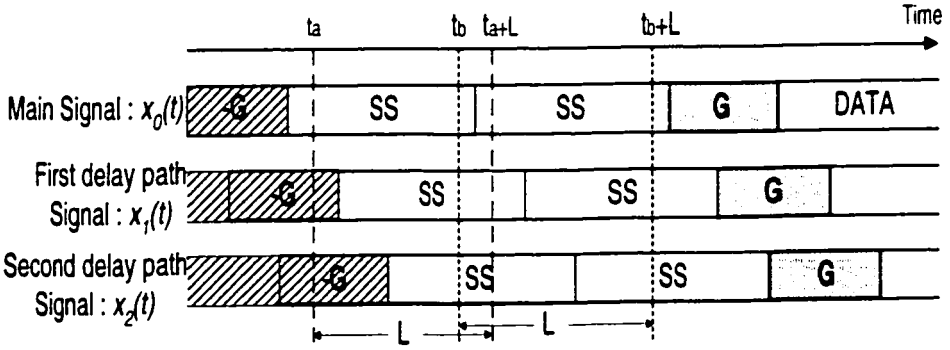

Figure 3.8 Problem of correlation calculation in a Multipath channel

The $P(d)$ and $R(d)$ corrected by weight function are given by

$$P(d) = \sum_{m=0}^{N-1} (r^{*}_{d+m} r_{d+m+N}) + \sum_{m=0}^{N-1} W(m) \cdot (r^{*}_{d+m} r_{d+m+N}) \tag{3.9}$$

$$R(d) = \sum_{m=0}^{N-1} (W(m) + 1) \left| r_{d+m+N} \right|^2 \tag{3.10}$$

Then, by substituting *P(d)* and *R(d)* into (3.6) a new timing metric *M(d)* is formed.

3.3.1.2 Carrier frequency offset estimation

As depicted in Figure 3.4, FO is estimated by two parts, ε_I (IFO) and ε_F (FFO). Obviously, the training symbol in [8][9] can find timing and ε_F. However, in order to estimate ε_I at least one more training symbol is needed for [8][9][10], though[10] does not touch this topic at all. Thus it reduces the bandwidth efficiency. With the purpose of saving bandwidth, [9] modifies the ε_F estimation part of Schmidl and Cox's method. However, they use the same symbol timing method of Schmidl and Cox so that their estimator suffers the same poor timing metric plateau which directly leads to a large error variance of frequency offset at low SNR.

On the contrary, with the proposed modified training symbol structure, the highly precise symbol timing is obtained. The advantage of our method is also represented on the aspect of bandwidth efficiency. Using the same training symbol the frequency offset can also be estimated, and the frequency estimator performance is much better than [9] and[8] at low SNR.

The sequence D_k in Table 3.1 (column three) enables us to estimate the carrier frequency offset in two steps with the same training symbol for timing. ε_F can be found firstly by the phase of $P(\hat{d})$ in (3.9) with $\hat{d} = d_{max}$ such that

$$\hat{V}_f = \frac{angle(P(\hat{d}))}{\pi} \tag{3.11}$$

This V_f must be compensated using $r_n' = r_n e^{-j2\pi \hat{v}_f n/N}$ before FFT. Then, after the cyclic prefix is removed, according to the FFT properties [5] the FFT output of the training symbol can be written as

$$\hat{X}_k = e^{j\theta_k} H_{Mod(k-2g,N)} \sqrt{2} X_{Mod(k-2g,N)} + W_k \tag{3.12}$$

where $\theta_k = \theta_0 + \frac{2\pi\varepsilon_0(k-2g)}{N}$, g is the index in the possible range of the position shifts. W_k's are the samples of DFT/FFT outputs of the AWGN channel. $2g$ shift is due to the preset zeros values in the odd positions of X_k. As in Table 3.1 (column three), D_k is differentially modulated between X_k and X_{k+2} in Table 3.1 (column two) as

$$D_k = \begin{cases} \frac{X_k}{X_{k+2}}, & k = 0,2,\ldots,N-4 \\ \frac{X_k}{X_0}, & k = N-2 \end{cases} \tag{3.13}$$

In (3.13), the D_k value at k=N-2 is modified comparing with the zero value as in[9]. If the timing and V_f have been compensated, the quotient $\hat{X}_k / \hat{X}_{k+2}$ is approximately equal to D_k except that it will be circularly shifted by $2g$ in the frequency domain due to the uncompensated V_f. Therefore, a metric can be found for the V_f estimation. The estimated V_f can be obtained by $\hat{g} = g_{max}$ which maximizes the metric

$$F(g) = \frac{\left| \sum_{k \in K'} \hat{X}_{Mod(k+2g,N)} D_k^* \hat{X}^*_{Mod(k+2g+2,N)} \right|^2}{\left(\sum_{k \in K'} \left| \hat{X}_k \right|^2 \right)^2} \tag{3.14}$$

where $K' = \{0, 1, \ldots, N-2\}$ and $2g$ spans the elements of K'. Therefore, $V = 2g + V_f$ can be estimated by

$$\hat{v} = \frac{\varphi}{\pi} + 2\hat{g}, \qquad \varphi = angle(P(\hat{d})) \tag{3.15}$$

3.3.2 Scheme two

In this scheme, timing error is much smaller even at very low SNR, and both timing and frequency offset estimation are robust.

In next section, the simulation result shows that the new designed bandwidth efficient timing estimator in scheme one outperforms the other ones in [8][9][10]. However, the error variance of timing estimator in scheme one is not smaller enough. The wide main lobe around timing metric peak causes the error variance flat at higher value. An example of the timing metric curve in a multipath channel for scheme one is shown in Figure 3.13.

To achieve the best robustness to timing offset in a multipath fading channel, a much more efficient method of timing recovery is to use match filter. The same type of the training symbols is used for the sake of frequency offset estimation. As depicted in Figure 1.9, a matched filter correlates the received signal with the known OFDM training symbol [*SS SS*], and the timing is found at the peaks of the matched filter output.

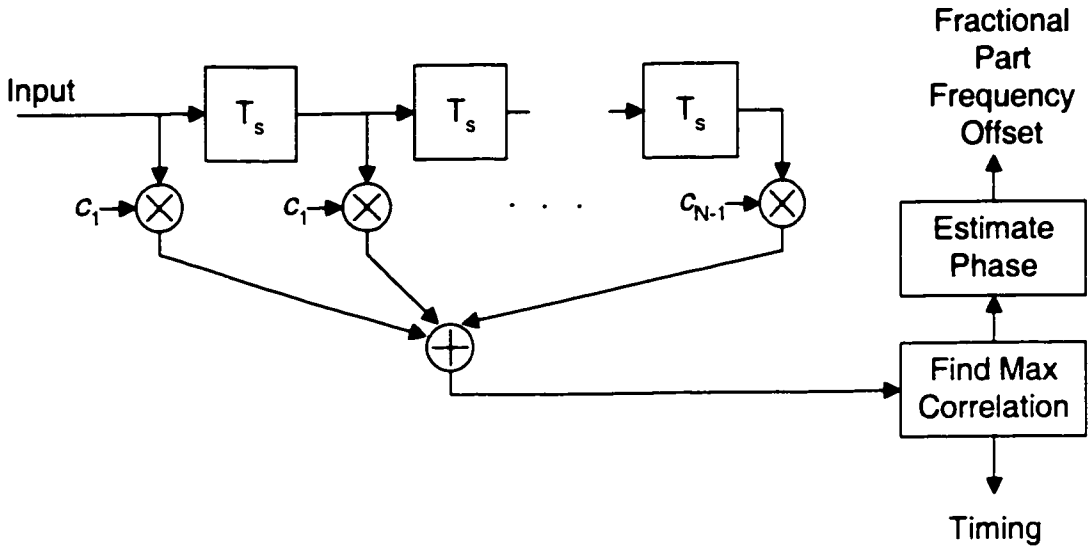

Figure 3.9 Synchronization using Matched filter

Here T_s is the sampling interval and c are the matched filter coefficients, which are in turn, the complex conjugates of the known training sequence. From the correlation peaks in the output signal, both the symbol timing and the frequency offset can be estimated. Frequency offset estimation shall employ the same method as in scheme one.

3.4 Simulation Result

The signals are affected by the Multipath channel in two ways, attenuation (fading) and delay. This section will compare the performance and also verify the robustness of above two new designed estimation schemes in Gaussian and time invariant multipath fading channel. In order to compare with two modified estimator schemes separately, we will use different system configurations as in [9][10].

3.4.1 Simulation Settings and Estimator Performance

First, for the timing offset estimation, the system is set as 1000 subcarriers with FFT size of 1024 points, 102 samples of the guard interval, QPSK modulation and carrier frequency offset ε of 12.4 subcarrier spacing and 10000 Monte Carlo simulation runs at each SNR. A 16 paths time invariant channel model with exponential multipath profile is employed with path delays τ_i of 0,4,8...60 samples. The path gains are $\rho_i = \rho exp(\tau_i / 30)$, where ρ_i is the power of the i-th path, and ρ meets $\sum_{i=0}^{16-1} \rho_i = 1$. In addition, α=*0.0*(for unweighted estimator) *or 0.8*(for improved weighted estimator) in scheme1.

Second, for the frequency offset estimation, the system is set as 1024 (FFT size) subcarriers, 64 samples of the guard interval, QPSK modulation and carrier frequency offset ε of 13.6 subcarrier spacing and 10000 Monte Carlo simulation runs at each SNR. The time invariant multipath fading channel is modeled as six paths with path delays τ_i of 0,10,20...60 samples and the path gains are also $\rho_i = \rho exp(\tau_i / 30)$. In addition, α=*0.0*(for unweighted estimator) *or 0.8*(for improved weighted estimator) in scheme1.

Table 3.2 summarizes the multipath performance in Figure 3.11 and Figure 3.12 for the overall comparison of all the different synchronization schemes used.

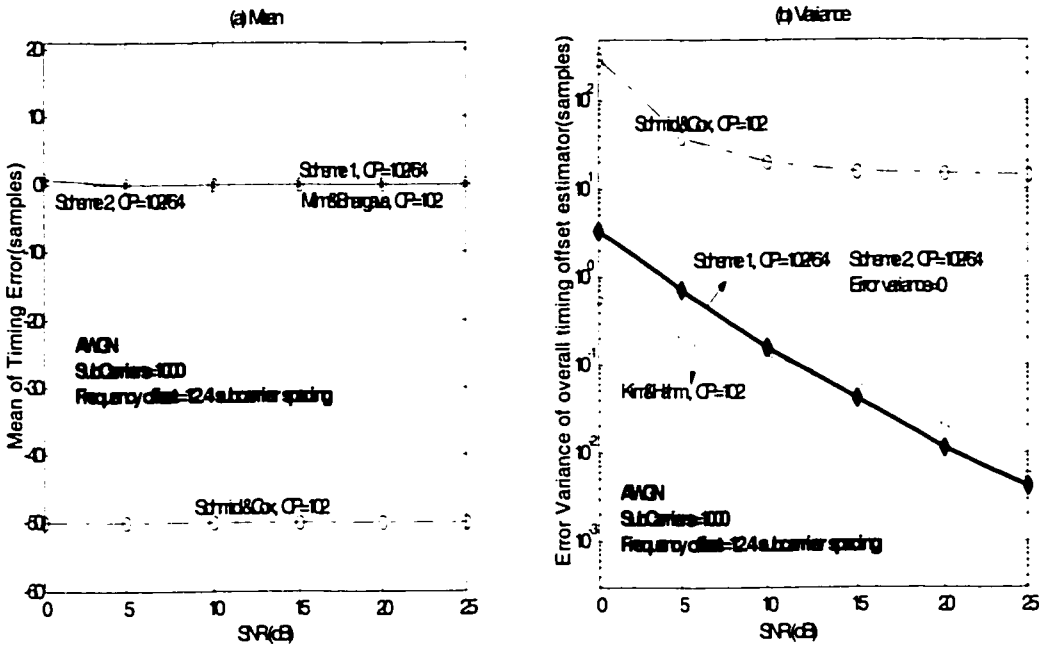

Figure 3.10 The mean and variance of symbol timing errors in AWGN channels

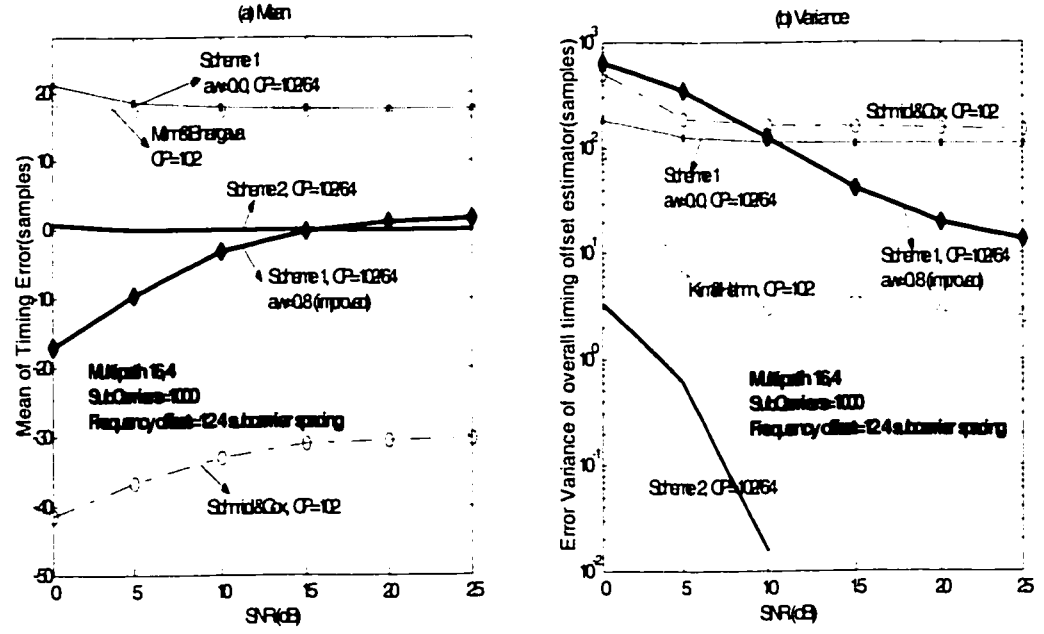

Figure 3.11 The mean and variance of symbol timing errors in Multipath channels

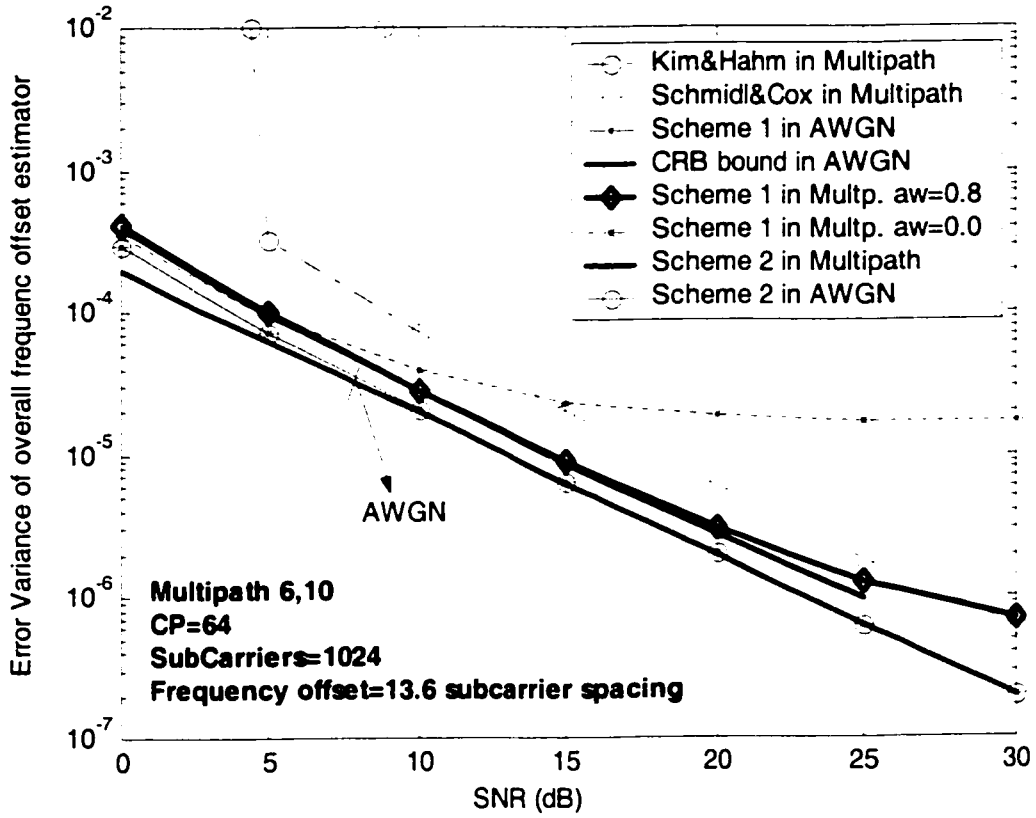

Figure 3.12 The error variance of frequency offset estimator

Estimation Schemes		Training symbol used (OFDM symbol)		Performance SNR = 0 ~ 25 dB (Approximate range)		
		Timing	*Frequency offset*	*Mean of timing error (sample)*	*Variance of timing error (sample)*	*Variance of frequency offset(sample)*
Schmidl&Cox[8]		1	1	-40~-30	4×10^{2} ~ 2×10^{2}	Very big at low SNRs (0~10dB)
Minn&Bhargava [10]		1	N/A	20 ~15	10^{2} ~ 2×10^{0}	N/A
Kim&Hahm [9]		1		Same as [7]	Same as [7]	Very big at low SNRs (0~5dB)
Proposed scheme I	a_w=0.0	1		20~15	2×10^{2} ~ 10^{2}	3×10^{-4} ~ 10^{-5}
	a_w=0.8			-15~5	6×10^{3} ~ 10^{1}	3×10^{-4} ~ 2×10^{-6}
Proposed scheme II		1		1 ~0	3×10^{0} ~ 0	3×10^{-4} ~ 1×10^{-6}

Table 3.2 Performance summary of the simulation in a 16-taps Multipath channel

3.4.2 Analysis of the Simulation Results

As shown in above Figure 3.10, the mean and variance of symbol timing errors for estimators in scheme one and [10] are more or less the same in AWGN channel, though the conventional Schmidl&Cox method deviates far. However, the mean and variance of the symbol timing errors for estimator in scheme two shows that there is no error for it in Gaussian channel.

In 16-taps multipath channel, the simple and efficient one training symbol based timing estimator proposed in [10] has the significantly smaller estimator error variance than the timing estimation algorithm in [8] both for AWGN and multipath channel. Similarly, the same level of accuracy on timing as in [10] was achieved by using scheme one when a_s=*0.0*. Comparatively, the further performance improvement of scheme one with the weighting function on mean of the timing error is deniable, though its timing error variance is slightly worse than the one in [10]. As for the estimator in scheme two, it achieves greatly smaller timing error variance and almost perfect timing even at low SNRs, which is unachievable for the methods in [8][10], and the estimator in scheme 1 are just secondary to it.

Furthermore, for both proposed estimators, there is still a potential to shorten the cyclic prefix. Even when the use of 102 samples [10] of guard interval is further reduced to 64 samples of guard interval, the discrepancy on the mean and variance of symbol timing errors is too small to be observed. This means the length of cyclic prefix could be further shortened as long as the cyclic prefix is longer than τ_{max}. Also, note that the timing estimator in [10] can be

used to estimate timing only and methods [8][10] need another training symbol to estimate the frequency offset, but using the same training symbol, ours two estimators can also estimate the frequency offset.

In AWGN channel, the error variance of all the frequency offset estimator is identical to the Cramer-Rao bound (CRB)[8]. By comparing the error variance of the frequency offset estimator in a 6-taps multipath channel, at low SNR, the two proposed estimator apparently gives the smaller error variance than[8][10] due to the more precise symbol timing estimation. In addition, Figure 3.12 shows that the variance of the frequency offset for the estimator in scheme two just slightly derivates from the CRB in Gaussian Channel. Therefore, estimator in scheme two is also the most robustness choice for the frequency offset thanks to its robustness on timing estimation.

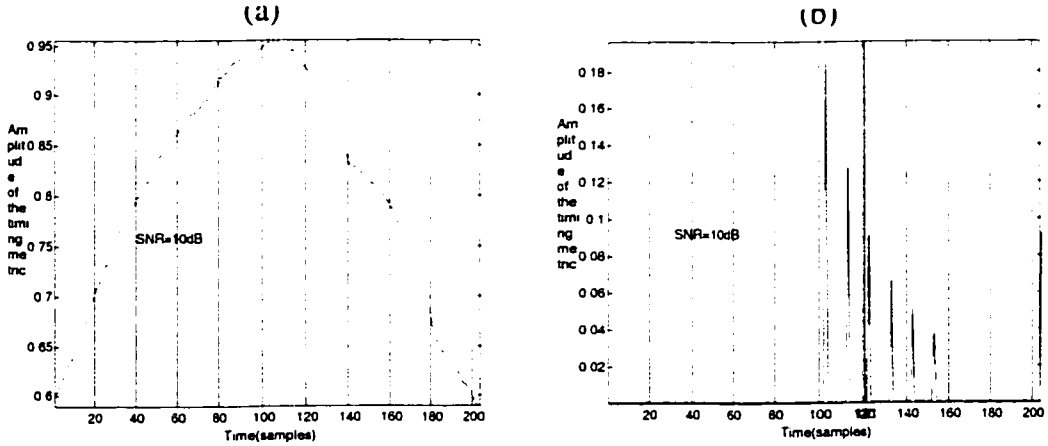

Figure 3.13 Timing metric in scheme one(Left) and scheme two(Right)

At last, in Figure 3.13, the plotting of the timing metric for both estimation schemes at SNR=10dB is given respectively. Obviously, the narrower main lobe around the peak and the

fast decay after in scheme two show its potential robustness in timing offset estimation compared with the too wider main lobes near the peak in scheme one. This leads to its overall excellent estimation performance.

3.5 Summary

In this chapter, two new efficient estimators have been presented using only one training symbol for two major synchronization issues of OFDM system. Both proposed estimators save not only bandwidth, but also give an improved accuracy. Due to their more accurate timing estimation, both have the potential to attain their best performance using less guard time. In addition, both schemes have the same frequency-offset estimator structure with a special redesigned training symbol and do not suffer the large error variance of the frequency offset. However, the timing estimator in the second scheme shows more robustness to multipath delay and also provides the smaller error variance of the frequency offset than the first one. As a result, in the following chapters, further investigation with coding and channel estimation will only be employed to the robust estimation scheme two.

Chapter 4

CHANNEL ESTIMATION

To cope with the unknown phase and amplitude variations of the constellation and enable the coherent detection at OFDM receiver, a simple channel estimation technique will be described in this chapter.

4.1 Channel Estimation for Coherent Demodulation

Channel estimation is simply defined as the process of characterizing the effect of the physical channel on the input sequence, and it is only a mathematical representation of what is truly happening. In a communication system training sequences are sent periodically to form data based estimates of the channel. The channel is also assumed to be invariant over the time span of the training sequence being sent over the channel.

Channel estimation algorithms allow the receiver to approximate the impulse response of the channel and explain the behavior of the channel. In a coherent OFDM receiver shown in Figure 4.1, after analog-to-digital conversion (ADC) and FFT, the coherent detection requires the knowledge of the random phase shifts and amplitude variations of the constellation on each subcarrier which are usually caused by the channel response, carrier frequency offset, timing offset and local oscillator shifts. Channel estimation is the technique to deal with them for dependable coherent detection.

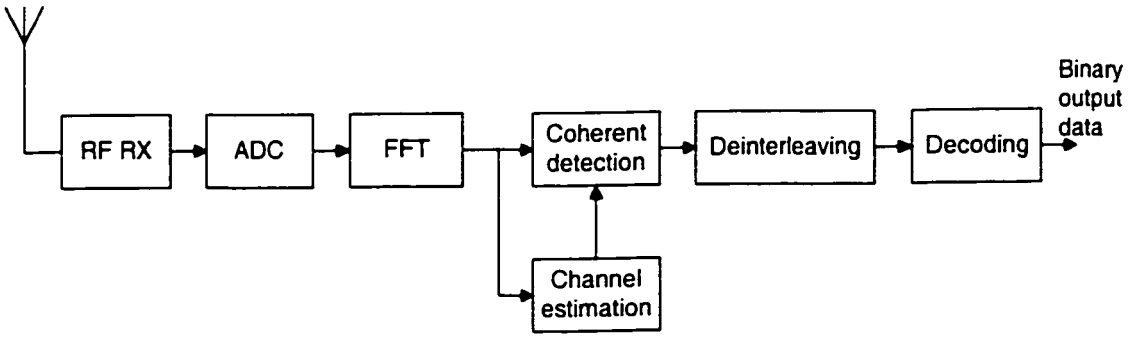

Figure 4.1 Block diagram of an OFDM receiver with coherent demodulation.

4.2 A Simple Channel Estimation Algorithm

There are several techniques to obtain the channel estimates existed for coherent detection in OFDM systems. Two–Dimensional channel estimators proposed in [26] perform a two dimensional interpolation to estimate points on a time-frequency grid based on several pilots. Instead of using a non-separable Two–Dimensional estimators, with the same complexity the use of two One–Dimensional channel estimators for time and frequency direction respectively is said to increase the performance a lot [23]. However, those estimators are designed for a channel that varied both in time and frequency, which are especially suitable for continuous transmission systems such as DAB or DVB.

For many packet oriented transmission systems in our case, those complicated channel estimation algorithms can be avoided. Firstly, there is no need to estimate time fading due to the constant channel during the short enough packet length. Secondly, the time delay introduced by using the scattered pilots over several OFDM data symbols is undesirable in packet transmission and also not unnecessary if time fading can be ignored. Therefore, an appropriate channel estimation approach is to use one or more known OFDM symbols as

preambles or training sequence. This method is called training sequence based Channel estimation algorithm.

A better BER performance can be achieved if more OFDM symbols are used for channel estimation. However, long training sequence is undesired. With the robust estimator in chapter three, the phase rotation caused by the timing estimation error has been mitigated to some extends. As a result, just one more known OFDM training symbol need to be added for a simple channel estimator. This is sketched in Figure 4.2. The grid with frequency subcarriers is on the vertical axis and the time grid with OFDM symbols is on the horizontal axis.

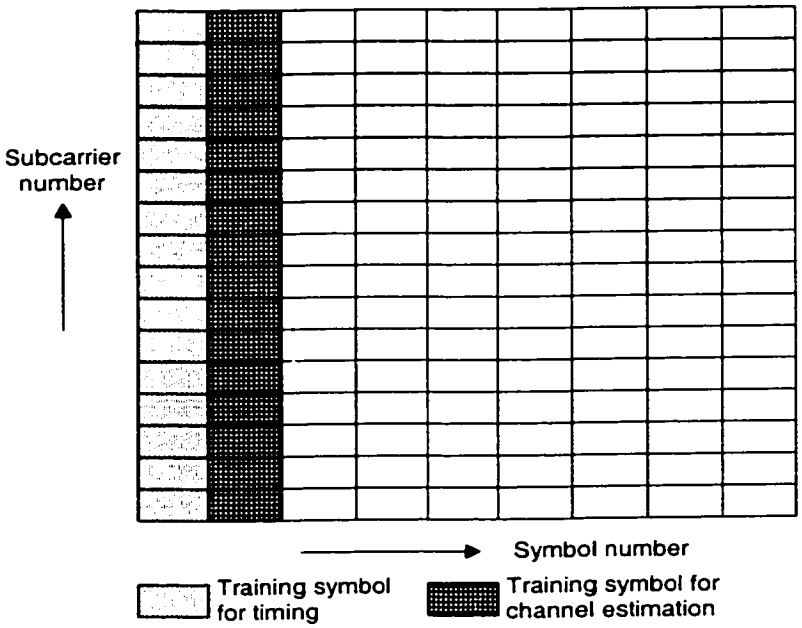

Figure 4.2 Example of a packet with two training symbols one for synchronization and one for channel estimation.

Based on the second known training symbol, the overall channel distortions then can be estimated simply by

$$\hat{H}_k = \frac{r_{2,n}}{X_{2,n}}; \qquad n = 0,1,2....N-1 \tag{4.1}$$

where $r_{2,n}$ is the received data symbols after FFT corresponding to the second training sequence and $X_{2,n}$ is the second known training sequence in the frequency domain. Compared with the complicated equalizer in a single carrier (SC) system, to correct the phase and amplitude distortions the OFDM system performs equalization by mean of a simple multiplier bank with the coefficients $\hat{H}_k$ estimated on each subcarrier in the frequency domain.

4.3 Simulation results

The timing and frequency offset estimation in scheme 1 and 2 outperform other training sequence based methods. As mentioned before, estimator in scheme 1 is not as robust as the one in scheme 2 over multipath channels, so it exhibits more server phase rotation and amplitude variations caused mainly by the timing errors. In this section, Figure 4.3 shows how important it is to estimate and compensate these channel distortions for scheme 1. In the simulation, the same six-path fading channel model established in the previous chapter is used. Figure 4.3 shows the BER performance regarding to the synchronization scheme 1 under two different assumptions.

- Assumption 1: Assume the channel response is known but the phase shifts and amplitude variations are unknown and not compensated.

- Assumption 2: Assume the channel response is known and phase shifts and amplitude variations are known and perfectly compensated.

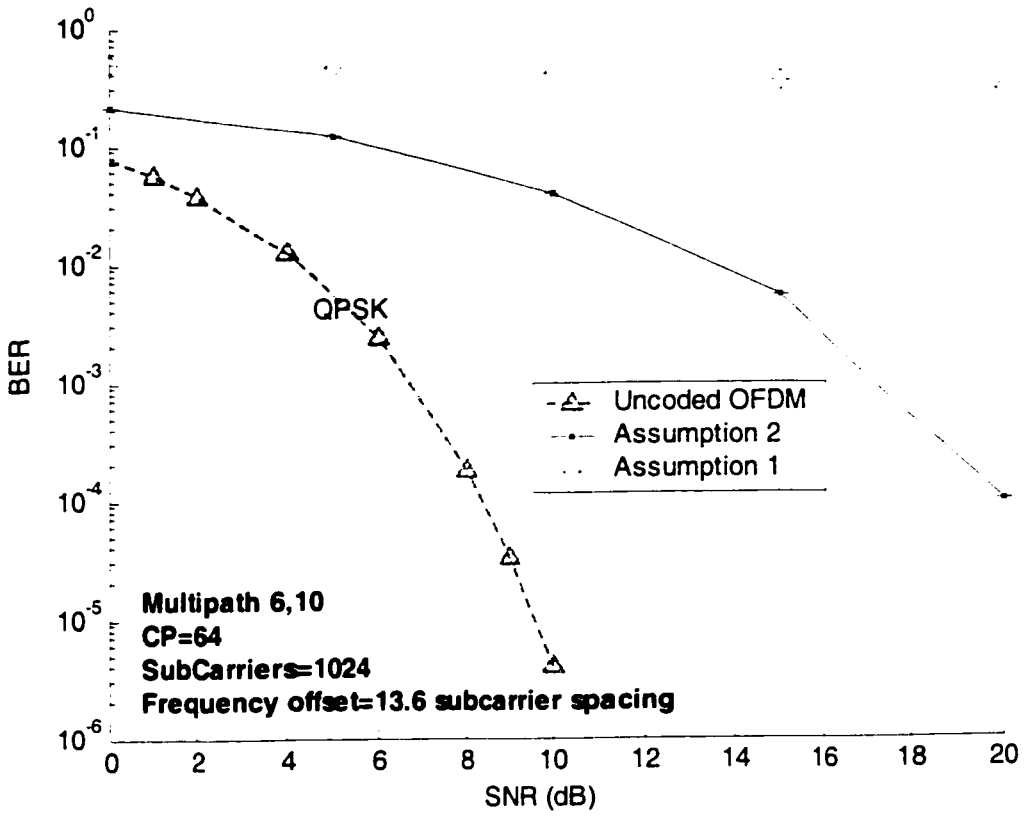

Figure 4.3 The important channel estimation in coherent demodulation.

Compare the two curves under the above two different assumptions, the curve with assumption two in the above figure shows a great gain for the multipath channel. Therefore, besides to estimate the multipath channel gain, the knowledge of the channel distortion caused by the residue timing offset is also very important in coherent demodulation OFDM systems. The above example is just to demonstrate the impact of the residue timing offset on channel distortions to be estimated. However, next, the channel estimation will be only applied to the chosen best synchronization scheme one.

For the robust timing and frequency offset estimators presented in chapter three, the BER performance after the overall channel estimation and compensation was investigated in multipath fading channels with the same system parameters described in chapter three. As seen in Figure 4.4 and Figure 4.5, for the two multipath fading channels there is only some small degradation by using the simple channel estimator compared to the curve with perfect synchronization and channel estimation.

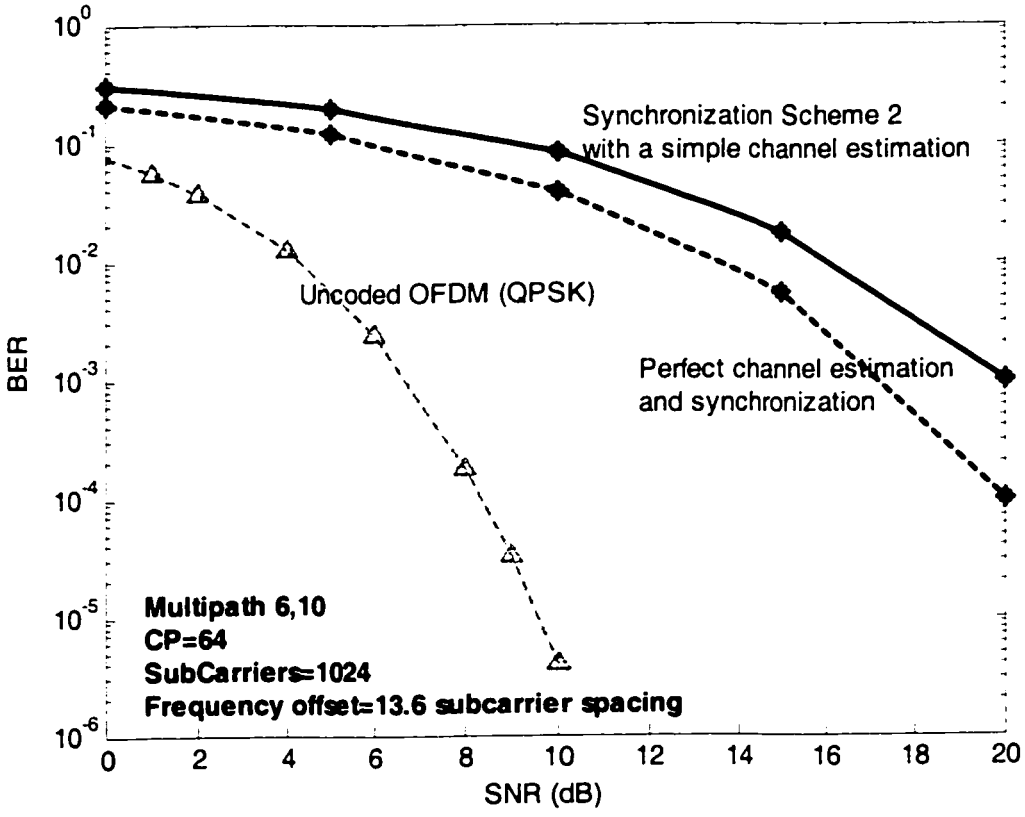

Figure 4.4 The BER performance in 6 taps Multipath channel with channel estimation and compensation.

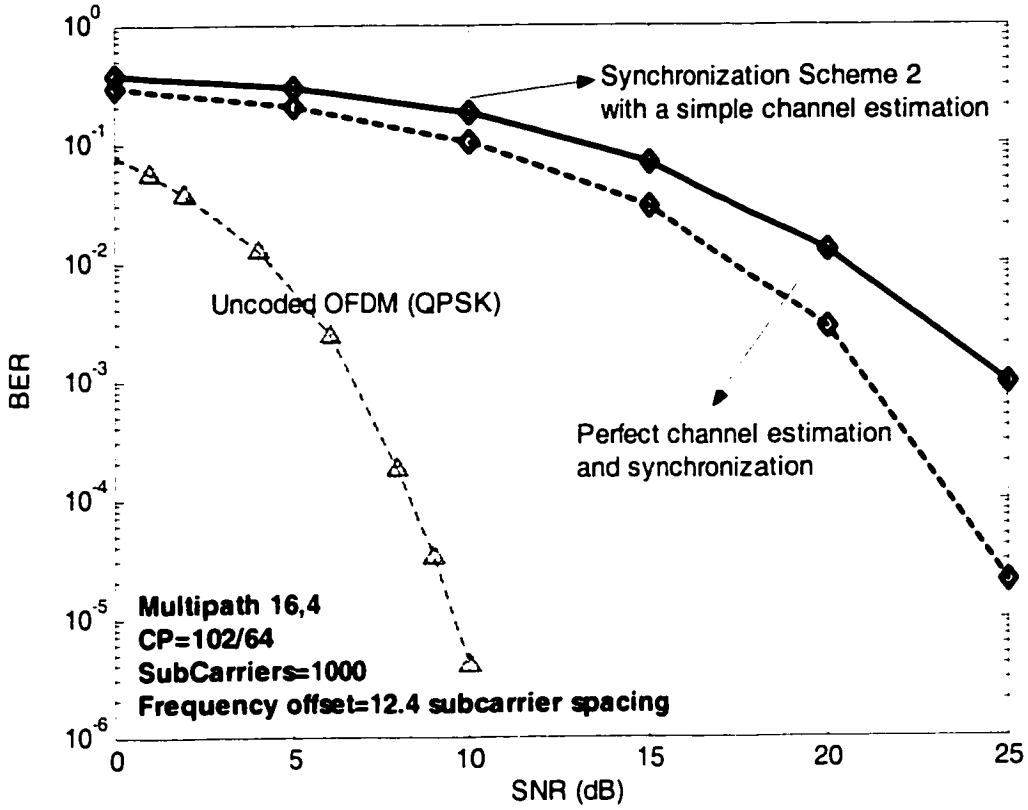

Figure 4.5 The BER performance in 16 taps Multipath channel with channel estimation and compensation.

4.4 Summary

The importance of getting the channel distortion knowledge for coherent demodulation at the OFDM receiver has been first illustrated in this chapter. Several of channel estimation schemes have been proposed in literature for OFDM systems. Some of them take long delays and also cost more in terms of hardware for buffering several OFDM symbols before getting the acceptable channel knowledge. Besides the lengthy time wait, the complexity of some kinds of channel estimation using scatter pilot tone is also high. Since the training sequence is available in packet transmission, the presented channel estimation

algorithm is a training sequence based channel estimation algorithm mainly used in packet-oriented wireless OFDM systems. Due to the robust estimator used for synchronization, only one more training symbol needs to be appended after the former training symbol for a simple channel estimation, and the phase and amplitude distortions have been well estimated and compensated.

Chapter 5

CHANNEL CODING FOR OFDM

In this chapter, an overview of different coding schemes for OFDM applications is given. Then, Turbo Convolution code (TCC) is introduced, focusing on optimizing its key design parameters, which significantly affect the code performance. For comparison, Turbo Product/Block code (TPC/TBC) is also discussed. Finally, overall system performance of the Turbo coded OFDM system in the multipath fading channel considering both channel estimation and synchronization is presented.

5.1 Overview of Coded OFDM

It is widely accepted that Forward Error Correction (FEC) channel coding is a valuable technique to increase both power and spectrum efficiency and improve the reliability in wireless communication systems. If channel coding is applied in our OFDM system, the performance of OFDM on fading channels is expected to be significantly improved through time diversity of channel coding as well as through inherent frequency diversity of the OFDM. In a multipath fading channel, if the data loss in a subcarrier occurs due to deep fade, it can be recovered from the coded data in alternative subcarrier channels, which may not suffer from the same level of fade distortion. As a result, the average power of the received signals shall determine the BER performance instead of the power of the subcarriers experiencing very low SNR.

Block codes, convolution codes and concatenated codes are all applied to OFDM in current relevant investigations. Block codes are hard decision codes and have not gained wide acceptance in wireless systems, since their performance does not reach the level of convolution codes. Convolution codes owe their popularity to good performance and flexibility to achieve different coding rates. Therefore, it is the most widely used channel code in practical wireless applications involving OFDM, as mentioned in Chapter one. Trellis-Coded Modulation (TCM) codes that is closely related to convolutional codes and algebraic Reed-Solomon (RS) codes was not selected as the coding method for IEEE 802.11a since for a practical high speed TCM system it would have to include some encoded bits in the encoder. However, it can be used optionally as the inner codes in concatenated codes that used to be the best performing error correcting codes. Several combination of concatenated codes applied to OFDM were studied in [18]. Concatenated codes built by combining the outer code an Reed-Solomon block code and an inner code a convolutional code have reached performance that is only 2.2 dB from the channel capacity limit. So, it is defined as one of the channel codes for COFDM in IEEE 802.16[17].

After about 50 years of research, Turbo-codes, which were presented to the coding community in 1993 [19], have finally emerged as a class of codes that can approach the ultimate limit, only 0.6 dB from the channel capacity, in performance. It has been shown to perform near the information capacity limits on deep space and satellite channels. Moreover, Turbo codes are particularly attractive to higher data rate application such as OFDM where the additional coding gain is necessary to maintain the link performance level with limited power. It is also proved that turbo coded OFDM is typically 2dB better performance over the RS

concatenated with a tail biting convolution codes. Consequently, as a powerful coding technique, turbo codes would also offer high coding gain in OFDM over fading channels.

A Turbo code is a parallel concatenation of two or more component codes separated by random interleavers. Either block codes or convolutional codes can be the component codes of Turbo codes. The term "turbo code" in the market today generally refers to Turbo Convolutional Codes (TCC). These codes are built by convolution codes as opposed to block codes which are used for Turbo product codes (TPC). In the next two sections it will be concentrated on them and then their performance in OFDM system.

5.2 Turbo Convolutional Codes

The initially introduced turbo codes are parallel concatenated convolution codes (PCCC) or Turbo convolutional codes (TCC). It is a combination of recursive systematic convolutional (RSC) codes, interleaving and iterative soft decision decoding. Encoder is formed by parallel concatenation of two recursive systematic convolutional codes joined by interleavers. The Decoder is Soft Input/Soft Output (SISO) decoder based on either a viterbi or MAP algorithm. A log maximum a posteriori (log-MAP) [11] algorithm is used in our simulation. There are a number of design parameters involved in determining the performance of turbo codes, such as the choice of component cods, memory size, interleaver design and the number of decoding iterations etc.

Since TCC used in the simulation is the most common type of turbo codes, the mathematical background is widely available in literature[12][19][22]. This section mainly investigates those key design parameters and their effect on selecting a TCC scheme that offers

the best performance for a specific system based on existing research journals and publications as indicated in the following subsections respectively.

5.2.1 Choice of constituent codes

The most common used constituent codes of TCC are RSC codes and the issue of choosing generator polynomials of the constituent codes is investigated in [28]. It is showed that the guidelines for choosing constituent codes are dependent on the target operating point of the code. Let us look at two different TCC constituent encoder structures and their state-diagrams, as shown in Figure 5.1, with generator polynomials (17/15) = $1+D+D^2+D^3/1+D+D^3$, and $(15/17)_8$ (both with no puncturing), where numerator and denominator are the feed forward (parity) and feedback polynomials respectively in octal representation. A single input '1' would cause the recursive encoder to cycle in a loop of states. Such zero-input loops are marked with solid lines. If there exists only one zero-input loop, the encoder is said to be with primitive feedback polynomials. Otherwise, it is the encoder with non-primitive polynomials. The length L of the longest zero-input loop corresponds to the periodicity of the infinite impulse response of the encoder, and it is also referred to as the period of the feedback polynomial. For the 8 state encoders in Figure 5.1, L is 7 and 4 respectively, and encoder (17/15) with the primitive feedback polynomial. The period L of the feedback polynomial highly influence on the distance spectrum of the TCC codes, especially, the minimum distance and the effective free distance. As demonstrated in [27], the best distance spectrum corresponds to the feedback polynomial with the longest period. Since primitive polynomials achieve the largest possible L for a given number of memory elements, the use of the primitive feedback polynomials is common in TCC literature.

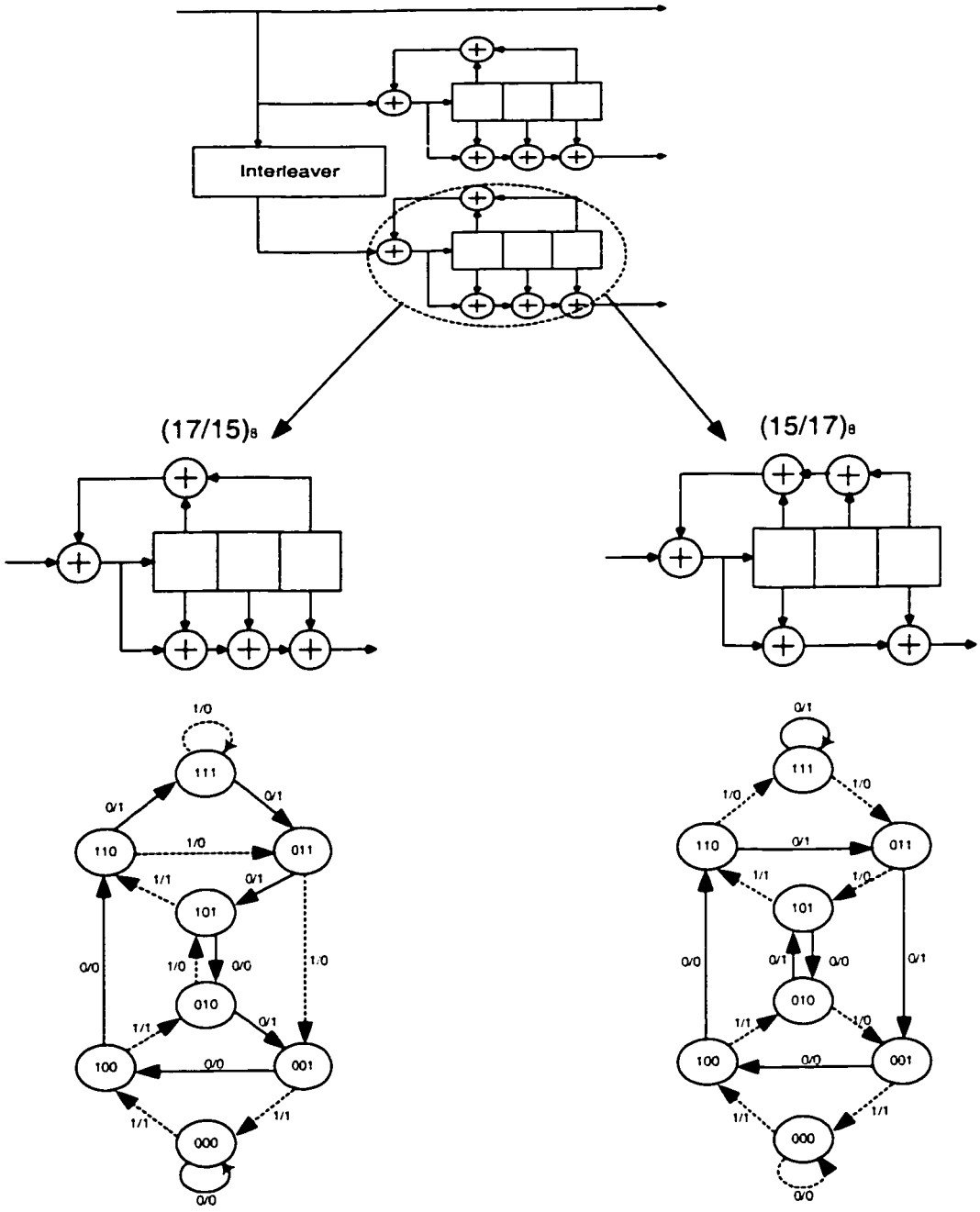

Figure 5.1 State diagrams of RSC encoder with generator polynomials $(17/15)_8$ and $(15/17)_8$, respectively. Zero-input loops are indicated by the solid lines

5.2.2 Constraint length K

One of the important measures in designing convolutional codes is the constraint length K, which is the maximum number of bits in a single output stream that can be affected by any input bit. In general, the constraint length is taken into be the length of the longest input shift register M (maximum memory order/size) plus one, K=M+1. Component codes with different constrain lengths (K) produce different results. For example, chosen the primitive feedback polynomials and given the same set of parameters, a 16-state (K=5) turbo code has a better performance than a 4-state (K=3) TCC code. Figure 5.3 demonstrates how the BER performance curves change for different number of states ranging from 4 to 16. Furthermore, increasing the maximum memory order/size doesn't affect the decoding delay. However, the computational complexity increases, and thus the implementation become more expensive.

5.2.3 Trellis termination

In the case of block-oriented Turbo codes, the constituent convolutional codes may be truncated at some unknown state. As a consequence, severe degradation of the error correcting performance may occur near the end of the trellis. One of the solutions to the above problem is trellis termination. With trellis termination, tail bits that terminate the encoder after encoding in the zero-state are appended to the information sequence. Numerous strategies and methods for trellis termination of turbo codes have been presented and proposed in the literatures [28][29][30]. In summary, the most common trellis termination methods are (1) Terminate the first encoder to zero-state;(2) Terminate the second encoder to zero-state; (3) Terminate both encoders to zero-state or No termination. And their relative

performances are investigated in [13]. The other approach to solve the trellis truncation problem is tail-biting. Tail-biting implies that the encoder is initialized and ended up to the same state. Since tail-biting does not require transmission of tail bits, it increases the code rate and the transmission bandwidth for small block size TCC codes. In our case, terminate the first encoder to zero state is a solution to avoid performance degradation due to unknown truncation.

5.2.4 Decoding iterations

Turbo codes use an iterative decoding algorithm. A relatively simple iterative decoding algorithm can achieve the superior performance of turbo codes compared with the complicated maximum likelihood (ML) decoding algorithm. As the number of iterations increases, the decoder performance improves. However, this performance improvement becomes negligible after a certain number of the iterations. As shown in Figure 5.5, the BER performance improves significantly after each iteration for the first six iterations, but from eight to ten iterations, the iteration gain turns small. Furthermore, after six iterations, increasing the signal to noise ratio does not impact the bit error rate and BER curve is almost flat at certain range of high SNR. This is often referred to as the "error floor" [31]. The bit error rate upper bounds presented in [32] can be used in estimating the "error floor." In the following sub-section through a study on interleaver used in TCC codes, this error floor will be well understood and further reduced.

5.2.5 Interleaver design

Interleaver rearranges the ordering of a symbol sequence, and the basic role of the interleaver is to construct a long random code. It has been widely used in error control coding,

particularly in the turbo codes, for channels with burst error characteristics. The interleaver in turbo codes is used to permute the input bits such that the constituent encoders are operating on the same set of input bits, but in different order.

The performance of the iterative decoder depends on both the size and the design of the interleaver. Figure 5.6 shows that the longer the interleaver size, the better the code performance is. However, long interleavers are used for high data rates because long interleavers introduce long delays, which are not desirable for lower data rates. Furthermore, since the iterative decoding algorithm assumes "uncorrelated" information exchange between the two constituent decoders, the interleaver should be scramble information data to the second constituent encoder so as to decorrelate the inputs to the two decoders. Moreover, the interleaving process changes the weight distribution of turbo codes. The above two target functions of interleavers are referred to the guidelines for the interleaver design.

There are a number of interleavers that have been used in TCC codes. The simplest block interleaver is a row and column interleaver [33], the data is written in rows and read by columns. The pseudorandom interleaver is a variation of the block interleaver in which the data is written sequentially and read out in a pseudorandom order [34]. In a convolutional interleaver, the data is multiplexed into and out of a fixed number of shift registers [35][36][37]. However, at medium to high SNR, for all these interleavers, the error floor is observed no matter which kind of constituent, how long the memory size and how much iteration is used. Even An improved "simile" interleaver [38], which terminates both constituent encoders in the same state, still can't eliminate the floor. Though using larger interleaver sizes can reduce the floor, it brings the intolerable longer latency and more power consumption. Of course, a

newclass of turbo codes such as the serial concatenated convolutional codes (SCCC) and Non-Binary Convolutional codes for turbo coding would be a good solution, but in fact a properly designed interleaver according to the above mentioned two guidelines could also perfectly eliminate the "error floor" typical for traditional TCC.

It is known that the asymptotic bit error probability is dominated by the code free distance [24]. Therefore, the flat curve at high SNRs is due to the relatively small free distance of turbo codes. From the analysis in [40][41] regarding the effect of the interleaver on the code distance spectrum, it is indicated in [42] that the error performance at medium to high SNR is determined by the first several spectral lines, which correspond to those low weight codewords. A good interleaver design based on the distance spectrum should be able to break low weight input sequence patterns, which produce low weight parity-check sequences at the first constituent encoders output, so that the input sequences to the other constituent encoder will generate high weight parity-check sequences. Thus the increased overall codeword weight and as well as the free distance, the error floor could be mitigated.

Recently, some work has been done in the interleaver design used to improve the code performance at high SNRs based on weight distribution of turbo codes. The S-random interleaver proposed in [39] is an improved version of the pseudo-random interleaver. It can "spread" low weight input patterns to generate higher weight codewords, hence can achieve better performance compared to pseudorandom interleavers. Furthermore, Based on the S-random interleaver, a code-matched interleaver [42] design in which is constructed to match the code weight distribution. The low weight paths caused by the input information sequences

with weights 2, 3, and 4 in the code trellis are almost eliminated so that thee "error floor" is lowered considerably compared with S-random interleavers.

However, unless the tail-biting or termination both encoders to zero-state, the truncation will leads to three types of interleaver edge effects corresponding to no trellis termination and two different trellis termination methods: terminate the first encoder to zero-state and terminate the second encoder to zero-state. Examples of interleaver edge effects lead to low weight codewords can be found in [16]. Because the code-matched interleaver doesn't take the interleaver edge effects into account, the code performance by using it might perform poorly as long as one or both of encoders is left unterminated. Fortunately, those interleaver edge effects can be avoided by the careful interleaver design, so that the performance of TCC will not be sensitive to the termination methods anymore. For example, considering the case that the first encoder is terminated to zeros-state. The interleaver edge effects are simply avoided by eliminating all the interleaver mapping, shown in [43], in the interleaver design.

Beside the good code weight distribution, the code performance is also depended on a good correlation property given by an interleaver design. Since in the derivation of the MAP algorithm, several assumptions regarding independencies between stochastic variables are made. Consequently, the interleaver will also play an important role on maintaining those independencies so that iterative decoding can make the effective soft decisions. In [21] a golden interleaver with very good correlation properties is proposed, but it often suffer from the error floor caused by the large number of relatively low-weigh codewords. This is depicted in simulation results. So, the good correlation properties combined with the good distance spectrum is very curtail to interleaver design.

A distance spectrum and correlation designed interleaver with both good correlation properties and distance spectrum is presented in[43] . The good correlation property is achieved by minimizing a mathematic approximation of the correlation function of those outputs, which should be independent to each other. In addition, the good distance spectrum is realized by the specific interleaver design (tailoring to the specific component code type and also the trellis termination methods) and the desired free distance can be set by the parameter d_{design}. Its detailed design procedures can be found in[43] .

5.2.6 Puncturing

Puncturing was firstly discovered by Cain, Clark, and Geist [14], and subsequently was improved by Hagenauer [15]. It is a very useful technique to generate different code rates. The basic idea behind puncturing is removing some of the bits from the encoder outputs, thus increasing the code rate. On the other hand, this increase in code rate decreases the free distance of the code so that it results in poor code performance and a higher noise floor for TCC. Figure 5.9 shows the performance degradation when the 1/3 code rate of TCC is punctured to half code rate TCC. Therefore, using TCC at higher code rate requires modifying the decoder. Alternately, TPC is preferred when much higher codes rates are desired.

5.3 Turbo Product codes

Unlike turbo convolutional codes, a turbo product code is a multidimensional array of block codes. It is a large code built from smaller code word blocks. Encoding is implemented as a binary block code on rows and then columns for 2-D codes. Decoding is also iterated several times to maximize performance of the decoder. Sometimes, in order to increase the

overall code rate, turbo product codes without parity on parity as shown in Figure 5.2 (b) are used. In this case, turbo product code can also be called turbo block codes.

5.3.1 Linear block codes

The component code of TPC/TBC is usually linear block codes. Linear block codes are characterized by $C(n,k)$ notation where n is the block length and k is the message length. The encoder transforms a block of k message symbols into a longer block of n codeword symbols. The redundancy contained in the n-k parity symbols provides the decoder with the necessary additional information to correct erroneous symbols.

Linear block codes used in TPC/TBC can be Extended Hamming codes and Reed Muller codes etc. Extended Hamming codes are a type of linear block code satisfied $(n,k)=(2^m,2^m\text{-}1\text{-}m)$ where integer m is greater than 1. One important characteristic of it is that they have a minimum Hamming distance of 4. The minimum Hamming distance determines the minimum error correcting capability of the code and a minimum Hamming distance of 4 means that the code can perfectly correct at least 1 error per codeword. When Extended Hamming codes are used in a 2-dimensional product code, the minimum distance of the overall code is 16 which ensures that the TPC codes will not suffer the error floor at moderate to high SNRs. Reed Muller codes have $n=2m$ and $k=1+\binom{m}{1}+\binom{m}{2}+\ldots+\binom{m}{r}$, where integer m is greater than 1 and the order of the Reed Muller codes r belongs to $[0,m]$. The minimum distance of RM codes is 2^{m-r}. By lowering the order of RM codes, it can have the variety of minimum distance other than 4 in Extended Hamming codes. So, when RM codes are used in a 2-dimensional product code, the minimum distance of the overall code is 4^{m-r}. For each m, by properly choosing the order r, Reed Muller codes equals to the corresponding Extended

Hamming codes with the same m. For example, the 3rd order RM codes for m=5, RM(32,26), is (32,26) Extended Hamming code.

5.3.2 Encoding and Decoding Procedures

Encoding is performed by placing the data in a k-by-k array. Each row and column is then encoded with the appropriate component code and the parity bits are appended to the end of each row. After all rows are encoded, the columns are encoded in the same manner resulting in an n-by-n coded array.

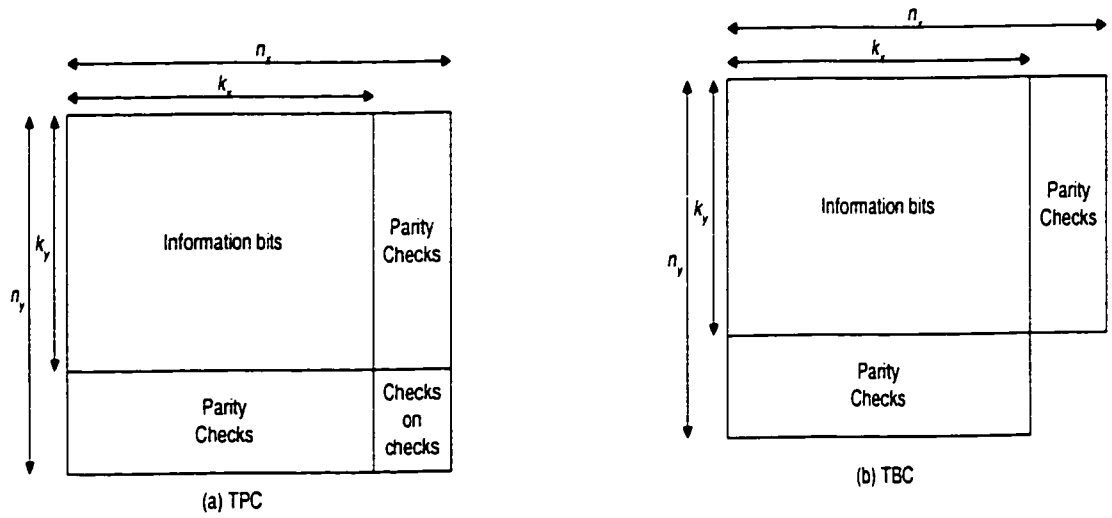

Figure 5.2 Two dimensional TBC/TPC.

The ideal method for 'turbo' decoding a product code array is to decode each row using soft decision correlation decoding. The output of the row decoding is then combined to the original data and input to a decoder for each column using soft decision correlation decoding. The output of the column decoding is input back to the row decoding. The process continues until the decoder settles on a valid transmitted code array or until the maximum

number of iterations is reached. Detailed Mathematical backgrounds can be found in literatures.

5.4 Simulation Results

5.4.1 Performance of TCC

Usually, when studying TCC, the two identical constitute codes are used.

5.4.1.1 Performance on the choice of constitute codes

First, primitive constitute codes 7/5, 15/17 and 35/23(all in octal, also in the following) with 4,8 and 16 states are used to investigate the effect of the memory size on the TCC performance. As shown in Figure 5.3, the BER performance of TCC with the larger state number constituent codes is better. However, this comparison is under the condition that the feedback polynomials of the constituent codes are primitive L=3, 7 and 15.

Then, by using the other 16 State constituent codes 21/37 with L=5 instead of 7/5. Figure 5.4 shows that the TCC using 16 state constituent codes 21/37 with L=5 performances worse than the TCC using 8 state constituent codes 15/17 but L=7. That means the performance of the TCC codes is determined not by the state number of the chosen constituent codes but the feedback polynomial period L. If the L are the same, nearly identical error performance are obtained for TCCs using the constituent codes with different number of state.

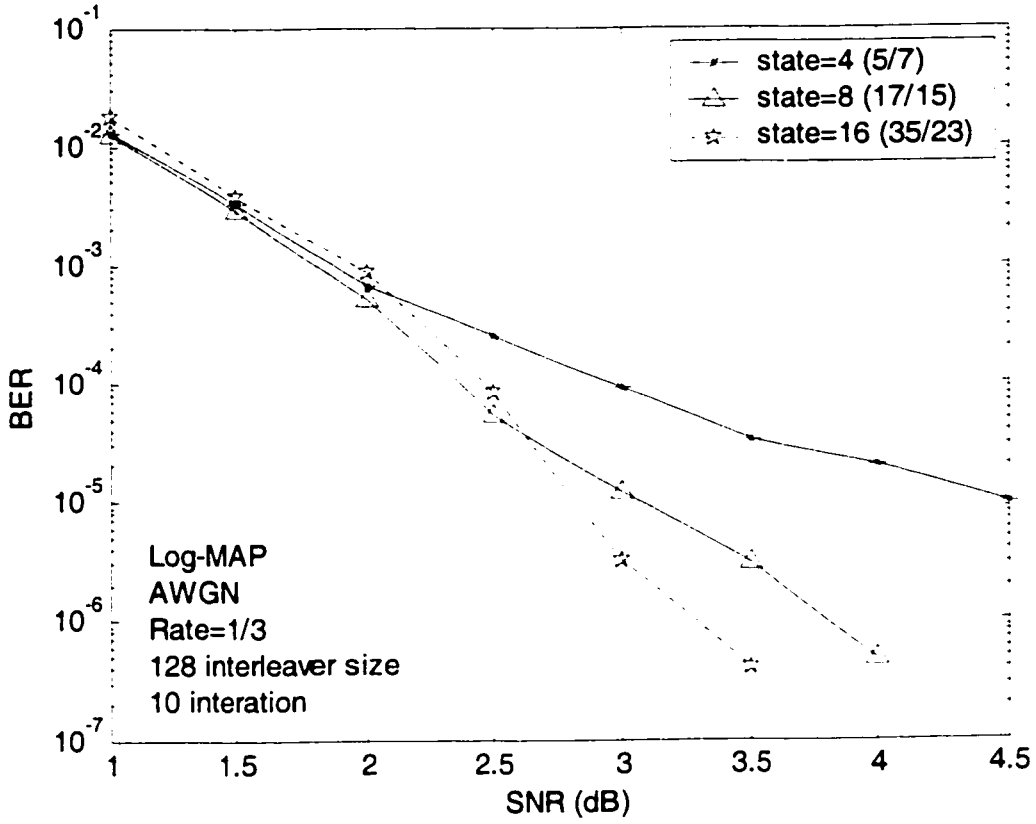

Figure 5.3 BER performance of state 4,8,16 constituent codes. (10 iteration and 128 random interleave size are used)

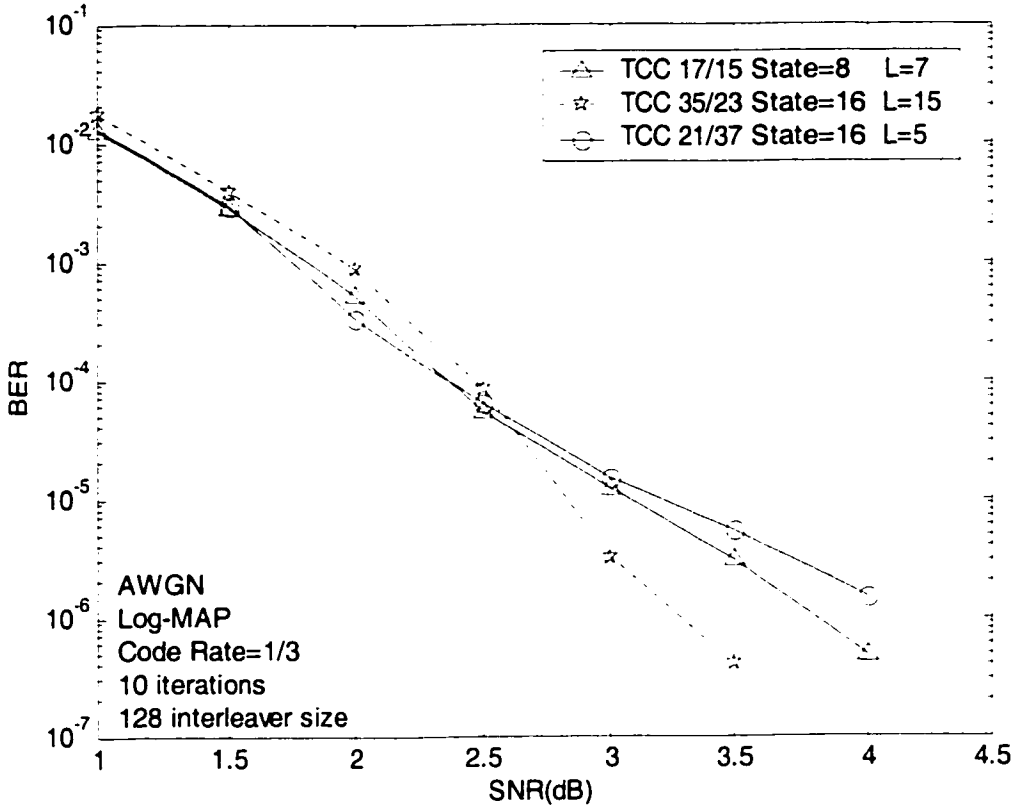

Figure 5.4 BER performance of state 8(L=7), 16(L=5,8) constituent codes. (10 iteration and 128 random interleave size are used)

5.4.1.2 Performance on iteration number

16 State constituent codes 21/37 with 1024 interleaver size and 10 iterations are simulated. Figure 5.5 show that the more the iteration, the better the TCC performances. However, this improvement is not obvious after 8 iterations. Usually, using 8 or 10 iteration is enough to get the good performance.

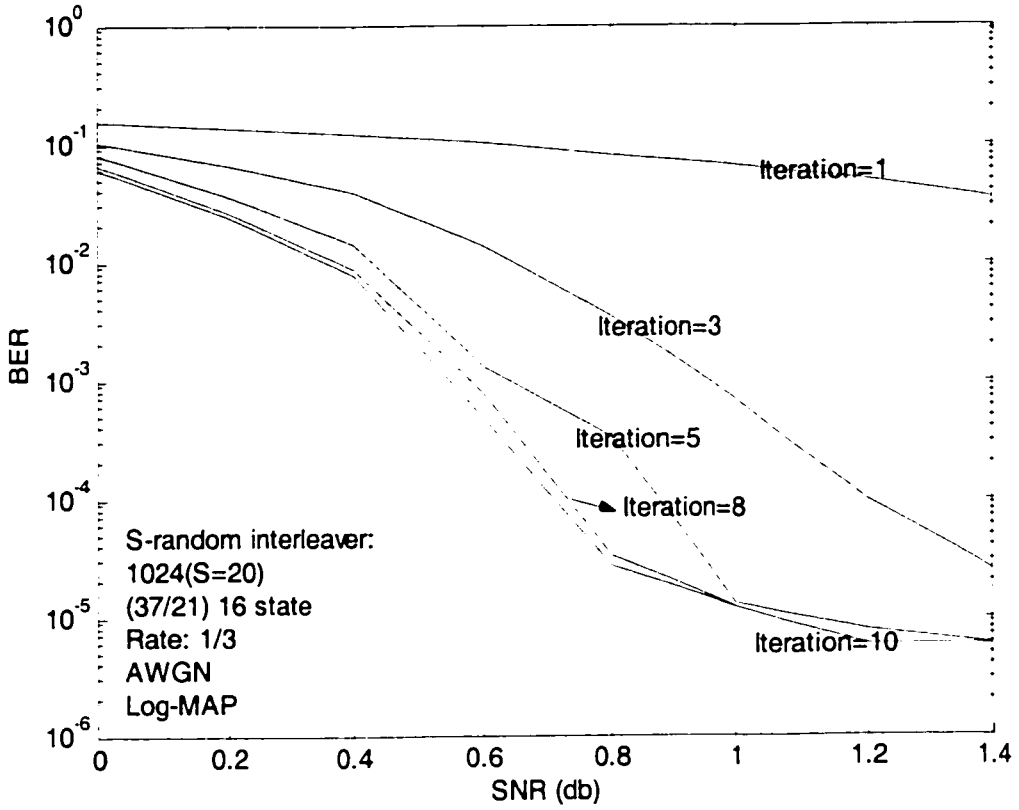

Figure 5.5 BER performance of constituent codes with iteration 1,3,5,8,10. (S-random interleave size 1024)

5.4.1.3 Performance on Interleaver design

First of all, different interleaver size 128,256, 512 and 1024 are used. 35/23 constituent codes is employed in the simulation, the iteration number used is 4.Figure 5.6 shows that the TCC performances better with larger interleaver size. However, this is a big cost for a system due to the long delay. Also, Note that none of the above discussed factors, which affect the TCC performance differently, effectively solve the performance degradation due to error floor.

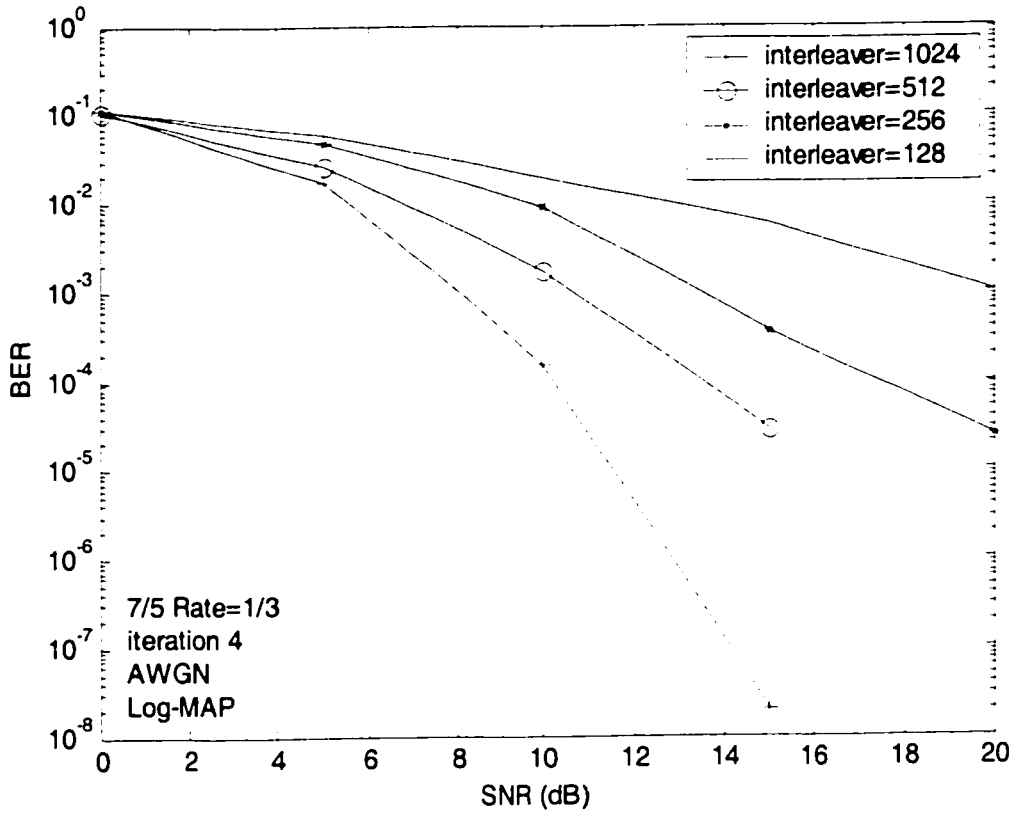

Figure 5.6 BER performance of interleaver size 128,256, 512 and 1024(4 iteration)

In addition, different interleavers, random, S-random Golden and correlation and distance spectrum designed interleavers, are used. 35/23 constituent codes is employed in the simulation, the iteration number used is 10. The permutation matrices of each types of interleaver in Figure 5.7 show that only golden and correlation and distance spectrum designed interleaver give symmetrical scatters which means good correlation prosperities. However, Golden interleaver suffers the error floor due to its poor weight distribution and minimum distance. S-random interleavers improve the distance spectrum of the random interleaver, but such improvement is just to lower the error floor and also it doesn't give a good correlation properties. Therefore, Figure 5.8 shows that only the correlation and distance spectrum

designed interleaver is outstanding and it doesn't suffer the error floor at all. Next, this special designed interleaver will be used in the simulation.

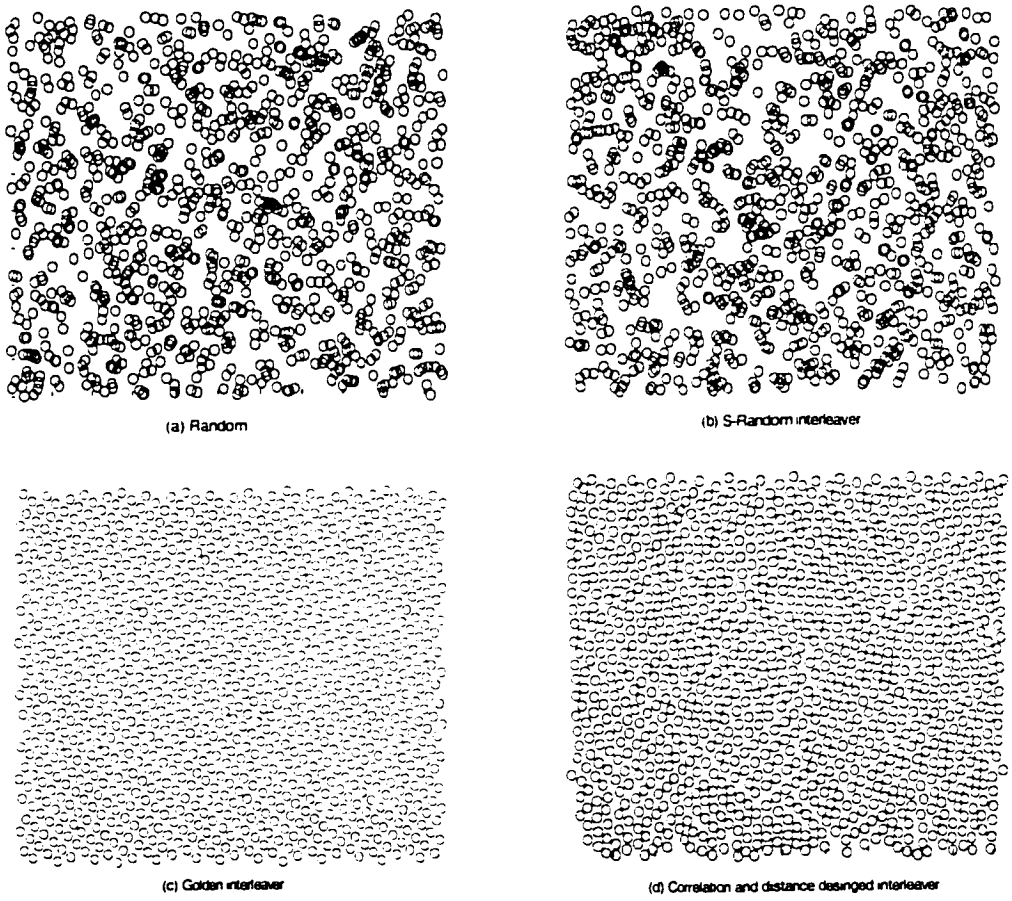

Figure 5.7 Permutation matrices of four different types of interleavers

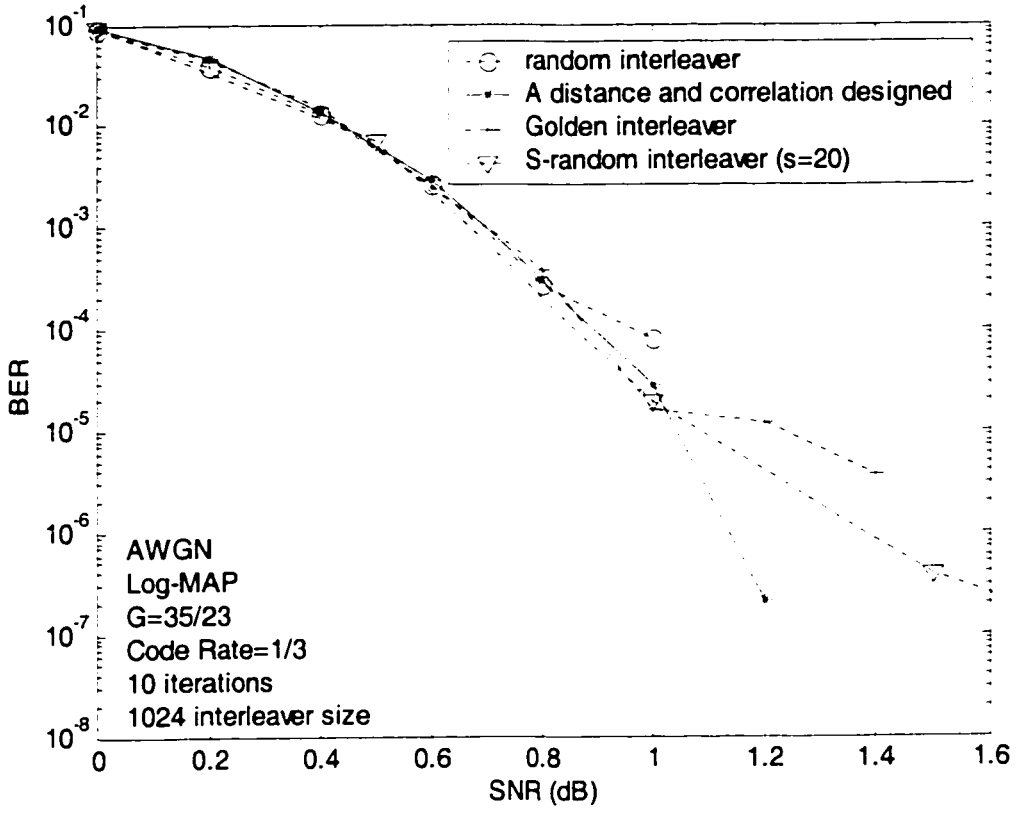

Figure 5.8 BER of four different types of interleavers

5.4.1.4 Performance with puncturing

With puncturing, the code rate of TCC can be increased from 1/3 to 3/4 or higher. If only the parity outputs on the odd/even position of the encoder one/two will be sent, the code rate of TCC codes can be increased to 1/2. Comparing the BER performance of the two different code rate TCC, it is obvious that the lower code rate TCC gives about 0.6dB gain than the higher rate TCC. The coding gain loss for the punctured higher code rate TCC is straightforward.

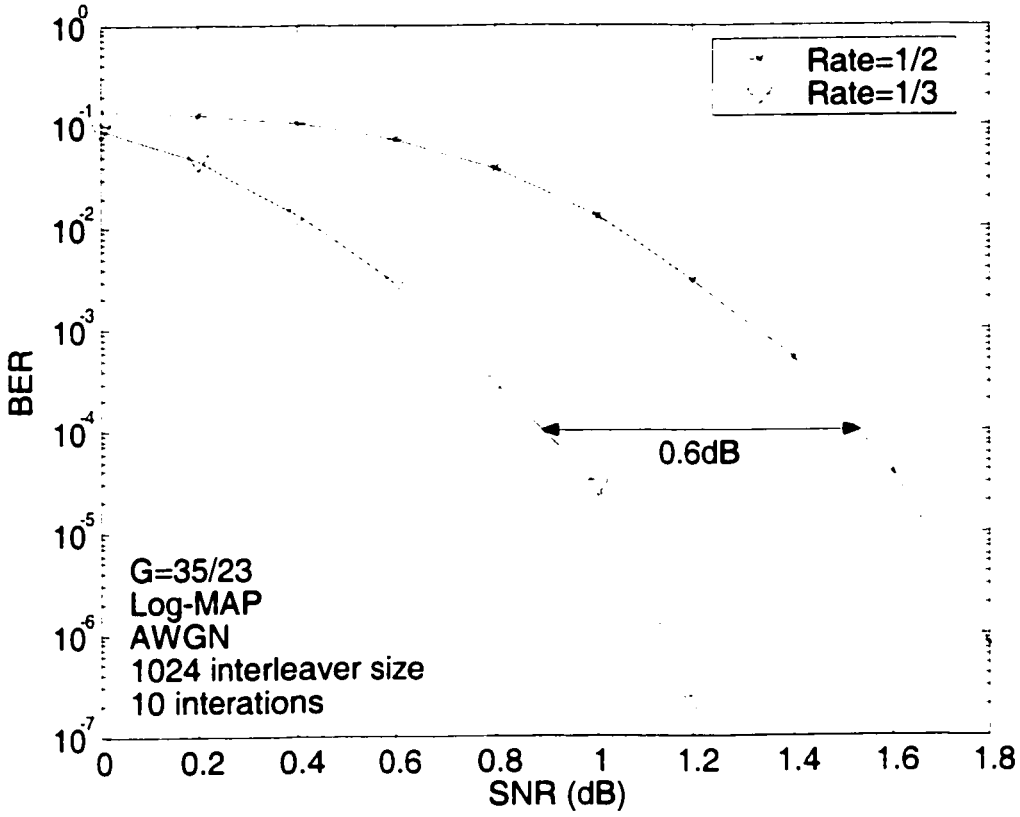

Figure 5.9 BER performance of puncturing

5.4.2 Performance of Turbo Codes for OFDM

TBC codes used here for comparison is RM(32,26)^2 with code rate 26*26/(32*32-(32-26)^2)=0.6842. According to the block size of TBC 32^2=1024 and its code rate, code rate 2/3=0.6667 TCC is used and the interleaver size is 680(block size 680*2/3=1020). Both use 5 iterations and are simulated with QPSK mapping in AWGN and multipath channels. Figure 5.10 shows that in AWGN channel 2/3 code rate TCC gives 0.5dB coding gain at BER=10^{-5} over the TBC at code rate 0.68. Further, let us assume that the receiver is perfectly synchronized to transmitter and also the channel is known. Then, in a 6-taps multipath

channel described in chapter 3, apparently, Figure 5.11 shows that code rate 2/3 TCC also shows better BER performance than TBC. Therefore, only TCC codes will be used in the next section.

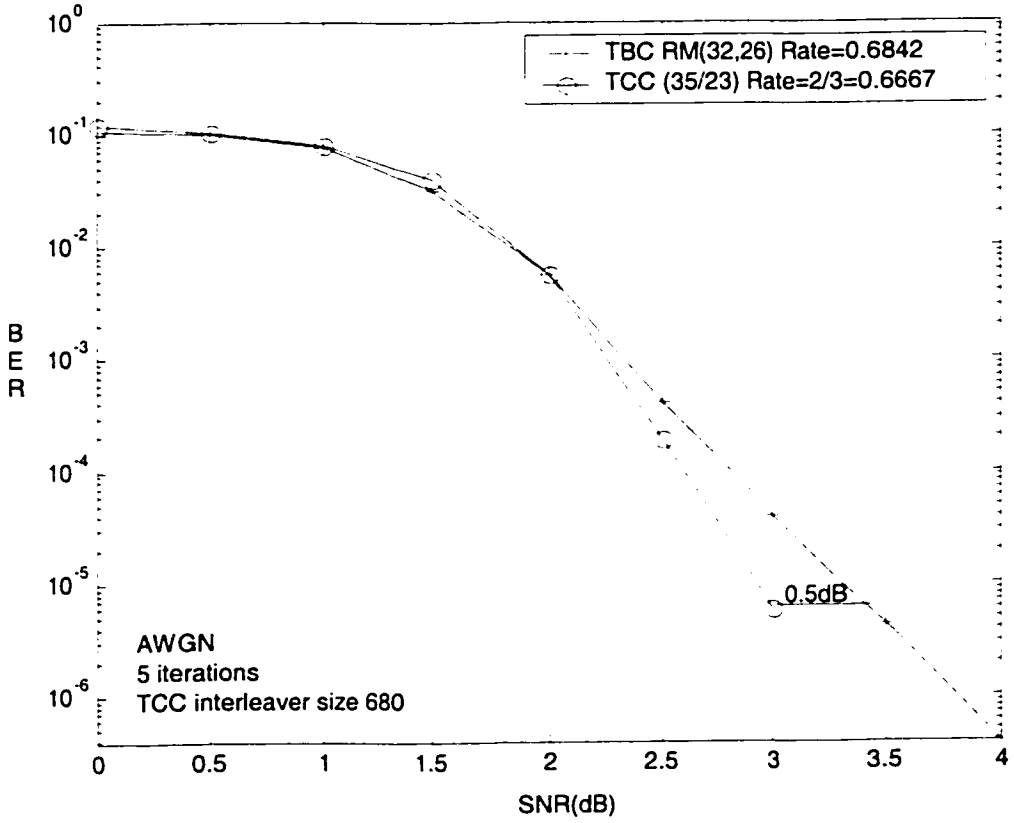

Figure 5.10 TBC vs. TPC in AWGN.

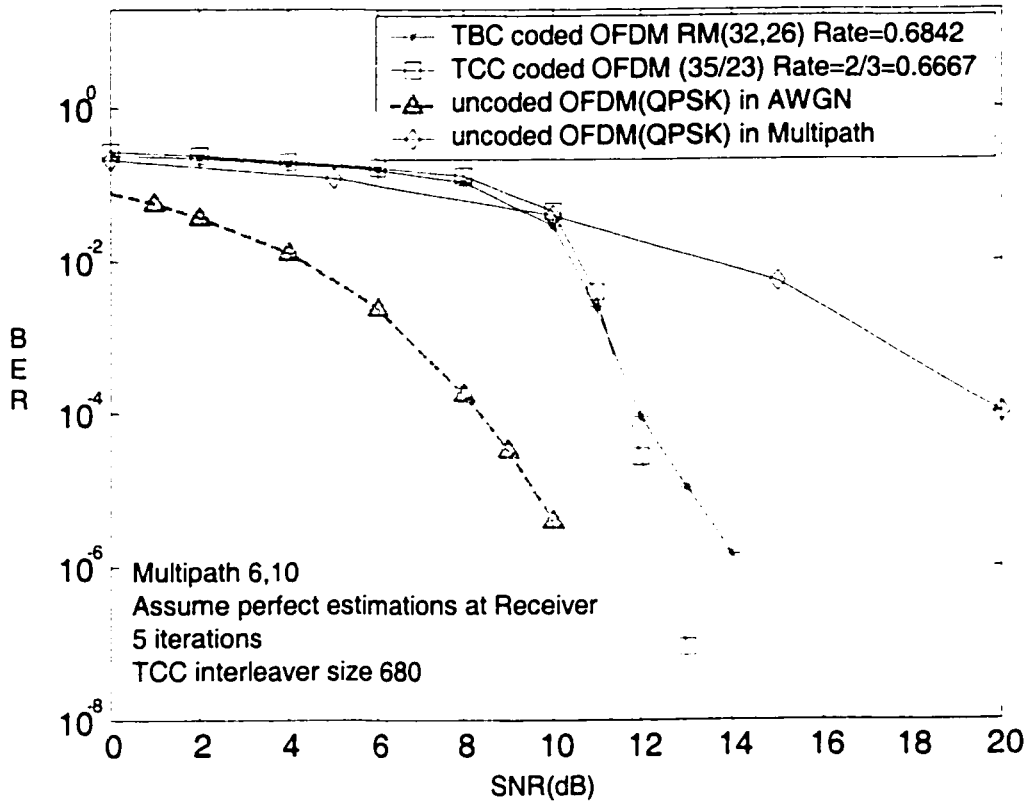

Figure 5.11 TBC vs. TPC coded OFDM in Multipath.

5.4.3 Performance of Turbo Coded OFDM with estimations

After the discussion about the channel estimation in chapter 4, in this section given generator polynomial 35/23, a code rate 1/2 TCC with the interleaver size 1024 and 10 iterations is used as the coding scheme for a complete OFDM baseband system. In Figure 5.12, assuming that the channel is perfectly known and the synchronization scheme 2 is applied at the receiver, the 10dB coding gains at BER=10^{-4} in both 6-taps and 16-taps Multipath channel make the OFDM system work more reliable and efficient. If considering the channel estimation instead of assuming the channel is known at the receiver, the BER performance of the complete COFDM system is shown in Figure 5.13. The simple and one

training symbol based channel estimation does bring some performance degradation even with coding. However, if necessary this degradation can be reduced by using two training symbols or increasing the complexity of the channel estimation algorithm. So there is a trade-off between the complexity of the channel estimation and the good overall performance.

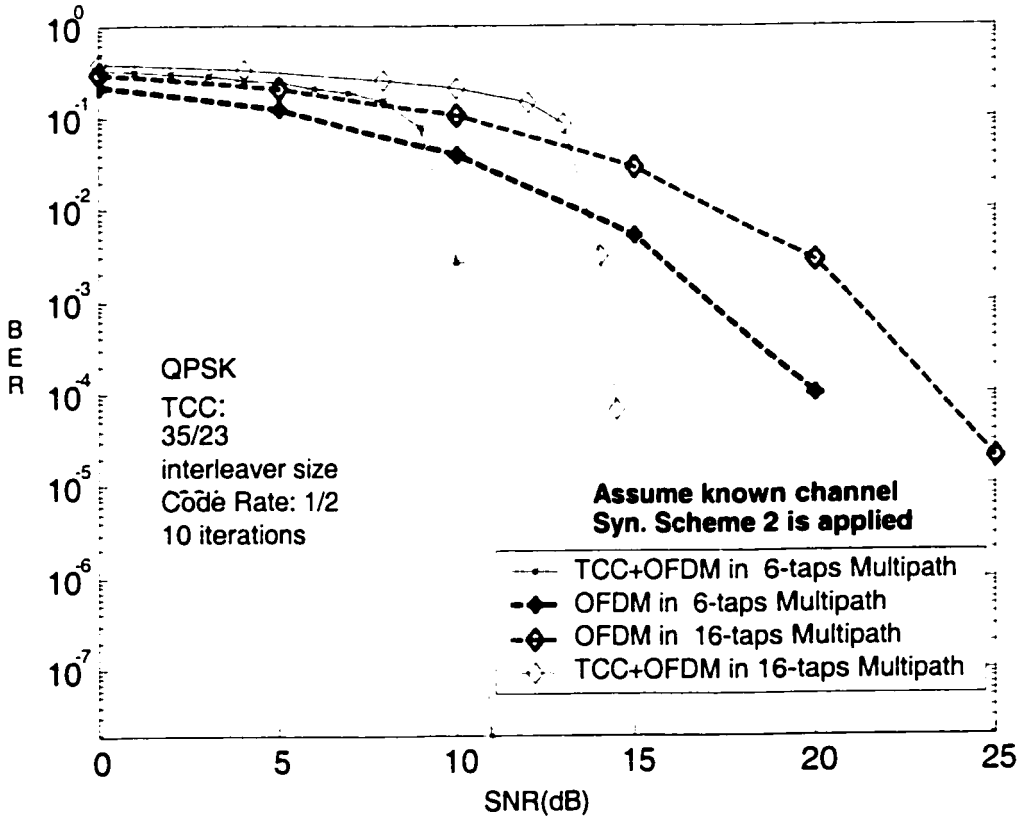

Figure 5.12 BER performance of COFDM in Multipath channels with synchronization scheme 2 and assume the channel is known

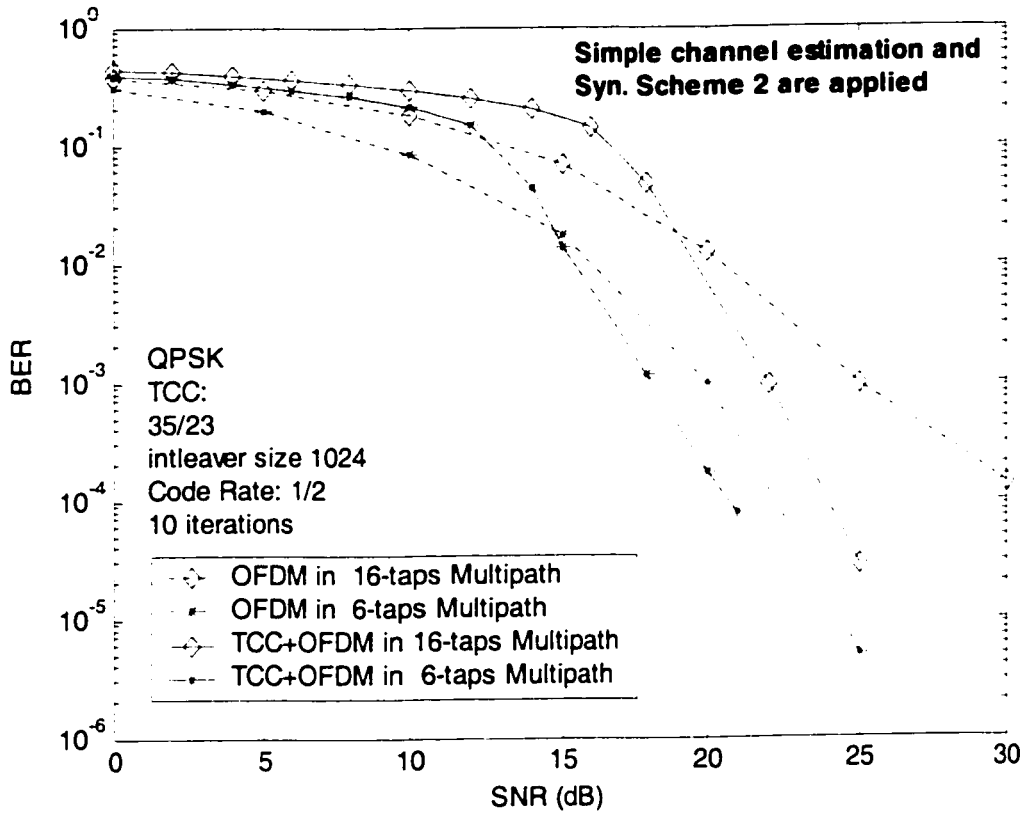

Figure 5.13 BER performance of COFDM in Multipath channels with both the synchronization and channel estimation

5.5 Summary

Provided a suitable guard interval is used, COFDM is particularly well matched to many kinds of wireless applications, since it is very tolerant of the effects of multipath. Among some of the widely used FEC schemes, the advanced turbo codes can be a best choice for OFDM systems. TPC/TBC and TCC are used to investigate COFDM system in Multipath channels. Due to a good correlation and distance designed interleaver, the typical error floor for TCC can be absolutely eliminated. At code rate 2/3 TCC outperformed than code rate 0.684 TBC with the similar block size in both AWGN and multipath channels. Therefore,

TCCs have been chosen to be investigated in a complete COFDM system. With synchronization scheme two and perfect channel estimation, 10dB coding gains of the TCC coded OFDM in multipath channel was also observed. Finally, the application of TCC channel coding to OFDM systems is a very promising approach to make full use of the merits of OFDM and channel coding schemes.

Chapter 6

Conclusion

6.1 Conclusion

In this thesis, the fundamentals of OFDM have been introduced first. Based on the mathematical backgrounds, the basic baseband OFDM system model has been established. By analyzing one of the major disadvantages of OFDM, an OFDM model with a novel synchronization algorithm has been developed. The novel synchronization scheme has been designed especially for packet oriented transmissions and displays its outstanding characteristics in terms of the bandwidth efficiency and precision. Next, channel estimation and channel coding together with the synchronization have been used to form a complete OFDM system. In addition to the robust synchronization scheme, the powerful coding scheme achieves further coding gain so that it makes the overall OFDM systems more immune to multipath propagation.

OFDM has several interesting properties such as high spectral efficiency, high data rates and robustness to multipath channel fading that make it suitable for wireless channels. The definition of the Orthogonal Frequency Division Multiplexing implies that it is a multicarrier system with overlapping orthogonal subcarriers. This orthogonality between the subcarriers is the main characteristic, which distinguishes it from the ordinary multicarrier

systems with low spectral efficiency. In principle, OFDM can achieve large delay spread tolerance at high bit rates by converting a single bit stream into N parallel bit streams and adding a guard time to each OFDM symbol. Furthermore, the high data rate provided by OFDM in wireless channels is unreachable for single carrier systems. In terms of complexity, the key difference between OFDM and single carrier transmission is FFT versus equalizer. Because of the recent developments in DSP and VLSI technology, OFDM with FFT has been several orders of magnitude less complex than the single carrier transmission with equalizer.

There are mainly two drawbacks with the transmission of OFDM. The large PAP ratio leads to the small power efficiency to OFDM systems, which can be solved by employing a special coding scheme, clipping and peak windowing, but this is not the case we have discussed here. The other limitation of OFDM in many applications is that it is very sensitive to the synchronization issues. Two main synchronization issues are timing offset and frequency offset. Due to the introduction of the cyclic prefix as a guard time, the system's requirements on symbol timing are much loose. But the forward timing errors will still lead to ISI. Aside from this, the frequency errors will easily destroy the orthogonality between the subcarriers and introduce the ICI. Therefore, both timing and frequency offset must be well estimated and compensated for in OFDM systems.

Many researchers have investigated solutions to conquer the weakness of OFDM on synchronization issues. There are two main methods in literatures discussing the synchronization techniques for OFDM systems. One of them is based on the cyclic prefix,

which fits many of the continuous OFDM applications such as DVB and DAB. Most of the burst packet-oriented transmissions, on the other hand, prefer the other technique using the training symbols. No matter what, the objective of the all the investigations is to design a synchronizer with the smallest error variance. Usually, a superior accuracy means the use of more training symbols, however more training symbol will decrease the system bandwidth efficiency. Therefore, there is another purpose for the study of synchronization methods: using the least possible overhead to find the highest possible precision.

With the above two purposes, we have proposed two new synchronization schemes and compared them with some of the good synchronizers found in literature. The first scheme is a modification of the existing synchronization algorithm. Compared with the conventional method [8] and two of its modifications [10], it saves more bandwidth by using only one training symbol to estimate both timing and frequency offsets. It also provides greatly improved timing accuracy, same as in [10]. However, this competitive accuracy on timing is still not good enough to be accepted in a real system. There were two solutions for it. One is to use the channel estimation to correct the phase rotation caused by the timing errors, but it is sub optimum. An optimum choice could be the second proposed synchronization scheme with a modification only on the timing estimation part. Instead of doing the correlation to find the timing peak between two repeated parts in one training symbol, the correlation in the second proposed method for timing is between one known OFDM training symbol and the received signals. In this way, by using the same single training symbol in the first proposed scheme, the second proposed scheme could estimate the timing almost perfectly. Due to its

high accuracy on timing recovery, the accuracy of its frequency synchronization has also been greatly improved. Therefore, the overall performance has shown that the second novel proposed scheme is the best robust synchronization technique in both AWGN and Multipath channels.

Channel estimation plays a very important role in a coherent demodulation. In case of OFDM, the channel estimation has to estimate both the channel gain and also the phase rotation caused by timing errors. One more training symbol has to be appended after the training symbol for the synchronization. Since the fading is flat during one OFDM symbol, the overall channel gains can be easily estimated by simple one tap equalization. This is much more simplified compared with the complex equalizer used in single carrier systems.

The application of suitable coding schemes in OFDM systems provides a diverse effect through exploitation of the multipath nature of the fading channel. Thus, Forward Error Correcting schemes should be used in the OFDM system to improve the performance. Turbo codes are one of the codes near the Shannon limits channel. Turbo Product codes (TPC)/Turbo block codes (TBC) and Turbo Convolutional codes (TCC) are widely used turbo codes. The error floor is typical for the traditional TCC at the SNR region of interest for practical communication systems. However, our detailed study has indicated that the key factor affecting this unexpected floor is the interleaver. By using a correlation and distance spectrum designed interleaver, this floor can be perfectly eliminated. Therefore, TCC and TCC coded OFDM has slightly outperformed the TBC with approximately the

same spectral efficiency. Finally, the TCC was chosen to be investigated in a coded OFDM system with our proposed novel synchronization technique. With known channels, it has given a considerable coding gain of 10dB at BER=10^{-4}, though relatively less coding gain has also been observed with a very simple channel estimation in COFDM. As a conclusion, the powerful coding scheme together with our proposed novel synchronization technique will definitely increase the reliability and efficiency for potential OFDM based broadband wireless applications.

6.2 Further Work

- Since the estimation used in this work is not blind (non-data aided), it may cost more bandwidth. Thus, it could be possible to investigate a more complicated algorithm for estimating timing, frequency offset and even the channel gains without training symbol in a short time. Though this will increase the complexity, it may be worth the effort considering the potential gains on the bandwidth efficiency. In addition, windowing could also employed to sharpen the edge of the OFDM spectrum.

- Here, we have not studied the other main drawback of the OFDM system, PAP ratio. From the power efficiency point of view, it could be investigated in future works.

- Aside from the turbo codes, there are also another new developing channel codes, such as Low Density Parity Check codes, which also provides the good performance near the

Shannon limits. Its performance with OFDM in multipath channel could be a good comparison with the turbo coded ones.

- In 1993 Linnertz et al. proposed MC-CDMA [44]. This is a combination of OFDM with Code Division Multiple Access (CDMA). It could be an interesting research topic.

- Finally, since OFDM is a promising technology for achieving high data rate transmission in a mobile environment, the applications of OFDM to high data rate mobile communication system should be a challenging research area.

Reference

[1] Pandharipande, "Principles of OFDM," A. IEEE Potentials, Volume: 21 Issue: 2 , April-May 2002 Page(s): 16 –19

[2] Eklund, C.; Marks, R.B.; Stanwood, K.L.; Wang, S. "IEEE standard 802.16: a technical overview of the WirelessMAN/sup TM/ air interface for broadband wireless access", IEEE Communications Magazine, Volume: 40 Issue: 6 , June 2002 Page(s): 98 -107

[3] Richard Van Nee, Ramjee Prasad, "OFDM for Wireless Multimedia Communications", Artech House Publishsers.

[4] May T., Rohling H, "Reducing the Peak to Average Power Ratio of OFDM Radio Transmission Systems", Proceedings of IEEE VTC '98, Ottawa, Canada, pp. 2474-2478, May 18-21, 1998.

[5] Alan V. Oppenheim, Ronald, "Discrete-time signal processing", 1989.

[6] Landstrom, D., "Symbol time offset estimation in coherent OFDM systems", IEEE International Conference on Communications, Vol.1, Page(s): 500 –505, 1999.

[7] P. Moose, "A Technique for Orthogonal Frequency Division Multiplexing Frequency Offset Correction," IEEE Trans. Comm., Vol. 42, No.10, pp. 2908-1914, October 1994.

[8] T. Schmidl and D. Cox, "Robust Frequency and Timing Synchronization for OFDM," IEEE Transactions on Communications, vol.45, Dec. 1997

[9] Y. H. Kim and Y. K. Hahm, "An Efficient Frequency Offset Estimator for Timing and Frequency Synchronization in OFDM Systems", IEEE Pacific Rim Conference on Communications, Computers and Signal Processing, pp.580-583, 1999.

[10] Minn, H. and Bhargava, V.K., "A simple and efficient timing offset estimation for OFDM systems", IEEE Vehicular Technology Conference Proceedings, VTC 2000-Spring Tokyo. 2000 51st, Vol. 1, pp. 51 -55, 2000.

[11] Robertson, P.; Villebrun, E.; Hoeher, "A comparison of optimal and sub-optimal MAP decoding algorithms operating in the log domain" P. Communications, 1995. ICC '95 Seattle, 'Gateway to Globalization', 1995 IEEE International Conference on , Volume: 2 , 1995 Page(s): 1009 -1013 vol.2

[12] D. Divsalar and F. Pollara, "Turbo codes for PCS applications," in IEEE International Conference in Communications, (New York,USA), 1995.

[13] Johan Hokfelt, Ove Edfors and Torleiv Maseng. "A Survey on Trellis Termination Alternatives for Turbo Codes," VTC'99, Houston, Texas, May, 1999.

[14] J. B. Cain, G. C. Clark Jr., and J.M. Geist, "Punctured Convolutional Codes of Rate (n-1)/n and Simplified Maximum Likelihood Decoding," IEEE Transactions of Information Theory, Vol. IT-25, pp. 97-100, January 1979

[15] J. Hagenauer, "Rate Compatible Punctured Convolutional Codes and Their Applications,"IEEE Transactions on Communications, Vol. COM-36, pp. 389-400, April 1988

[16] Johan Hokfelt, Ove Edfors and Torleiv Maseng. "Turbo Codes: Interaction Between Trellis Termination Method and Interleaver Design," *RVK'99* Radio Science and Communications Conference, Karlskrona, Sweden, June, 1999.

[17] IEEE.802.16 Standard

[18] http://www.comlab.hut.fi/opetus/311/ofdm.pdf

[19] C. Berrou, A. Glavieux, and P. Thitimajshima, "Near Shannon limit error-correcting coding and decoding: Turbo-codes(1)," in Proc.ICC'93, May 1993, pp. 1064–1070.

[20] Weinstein.S. B, Ebert P.M, "Data Transmission by Frequency Division Multiplexing using the Discrete Fourier Transform", IEEE Transactions on Communications, Vol-COM-19, pp. 628-634, Oct 1971.

[21] S. Crozier, J. Lodge, P. Guinand and A. Hunt, "Performance of Turbo Codes with Relative Prime and Golden Interleaving Strategies", *Sixth International Mobile Satellite Conference (IMSC '99)*, (Ottawa, Canada, June 1999), pp. 268-275.

[22] C. Heegard and S. B. Wicker, "Turbo codes," Kluwer Academic Publishers, 1999

[23] M. Sandell and O. Edfors. "A comparative study of pilot-based channel estimators for wireless OFDM." Research Report TULEA 1996:19, Div. of Signal Processing, Luleå University of Technology, Luleå, Sept. 1996.

[24] S. Lin and D. J. Costello, "Error Control Coding: Fundamentals and Applications," Prentice-Hall, New Jersey, 2.ed, 1983

[25] J. G. Proakis, "Digital Communications," McGraw-Hill, Boston, 3ed., 1995

[26] Van de Beek, J.-J.; Edfors, O.; Sandell, M.; Wilson, S.K.; Borjesson, P.O, "On channel estimation in OFDM systems" Vehicular Technology Conference, 1995 IEEE 45th , Volume: 2 , 1995 Page(s): 815 -819 vol.2

[27] S. B. Wicker, "Error control coding," Prentice-Hall, New Jersey, 1995

[28] S. Benedetto,R. Garello, and G. Montorsi. "A search for good convolutional codes to be used in the construction of turbo codes." IEEE Transactions on Communications, 46(9):11101-1105, Sep. 1998.

[29] Barbulescu, A.S.; Pietrobon, S.S. "Terminating the trellis of turbo-codes in the same state." Electronics Letters, Volume: 31 Issue: 1, 5 Jan. 1995 Page(s): 22 -23

[30] Joerssen, O.; Meyr, H. "Terminating the trellis of turbo-codes." Electronics Letters , Volume: 30 Issue: 16 , 4 Aug. 1994 Page(s): 1285 -1286

[31] Perez, L.C.; Seghers, J.; Costello, D.J., Jr. "A distance spectrum interpretation of turbo codes." Information Theory, IEEE Transactions on , Volume: 42 Issue: 6 Part: 1 , Nov. 1996 Page(s): 1698 -1709

[32] D. Divsalar, S. Dolinar, F. Pollara, and R. McEliece, "Transfer function bounds on the performance of turbo codes," TDA Progress Rep., vol. 42-122, pp. 44–55, 1995.

[33] G. C. Clark, Jr. and J. B. Cain, Error Correction Coding for DigitalCommunications. New York: Plenum, 1981.

[34] I. Richer, "A sample interleaver for use with viterbi decoding," IEEE Trans. Commun., vol. 26, pp. 406–408, Mar. 1978.

[35] J. L. Ramsey, "Realization of optimum interleavers," IEEE Trans. Inform.Theory, vol. 16, pp. 338–345, May 1970.

[36] G. D. Forney, Jr., "Burst correcting codes for the classic bursty channel,"IEEE Trans. Commun., vol. 19, pp. 772–781, Oct. 1971.

[37] E. K. Hall and S. G.Wilson, "Convolutional interleavers for stream oriented parallel concatenated convolutional codes," in Proc.ISIT'98, Aug.1998, p. 33.

[38] A. S. Barbulescu and S. S. Pietrobon, "Terminating the trellis of turbo codes in the same state," Electron. Lett., vol. 31, pp. 22–23, 1995.

[39] D. Divsalar and F. Pollara, "Turbo codes for PCS applications," in Proc. ICC'95, Seattle, WA, June 1995.

[40] S. Benedetto and G. Montorsi, "Unveiling turbo codes: Some results on parallel concatenated coding schemes," IEEE Trans. Inform. Theory, vol. 42, pp. 409–428, Mar. 1996.

[41] Benedetto, S.; Montorsi, G., "Design of parallel concatenated convolutional codes," IEEE Trans. Commun., vol. 44, pp. 591–600, May 1996.

[42] J. Hokfelt and T. Maseng, "Methodical interleaver design for turbo codes," in Proc. Int. Symp. on Turbo Codes and Related Topics, Brest, France, Sept. 1997, pp. 212–215.

[43] Johan Hokfelt. On the Design of Turbo Codes. Ph.D. thesis. ISSN1402-8662:17, ISBN 91-7874-061-4, Lund University, Sweden, August 2000.

[44] N.Yee, J.-P.Linnartz und G.Fettweis, Multi-Carrier CDMA in Indoor Wireless Radio Networks, PIMRC,1993